Lucía Picazo Selva

Development and Implementation of Reactive Species Detection Systems in Plasma-Based Medicine Applications

Degree Final project

Director: Jan Mitrovics

Tutor: David Girbau

Bachelor's Degree in Biomedical Engineering

UNIVERSITAT ROVIRA i VIRGILI

Tarragona
2022-2023

Index of Acronyms

RONS	Reactive Oxygen and Nitrogen Species
PAL	Plasma Activated Liquid
3D	Three Dimensions
CNC	Computer Numerical Control
CEO	Chief Executive Officer
MCU	Microcontroller
MOX	Metal Oxide Semiconductor
MEMS	Micro Electro Mechanical Systems
PCB	Printed Circuit Board
PAM	Plasma Activated Medium
CAP	Cold Atmospheric Plasma
DC	Direct Current
DBD	Dielectric Barrier Discharge
H2O2	Hydrogen Peroxide
NO2	Nitrogen Dioxide
NO3	Nitrogen Trioxide
ONOO-	Peroxynitrite
EC	Electrical Conductivity
TDS	Total Dissolved Solids
PAW	Plasma Activated Water
DI	Deionized
1O2	Singlet Oxygen
-OH	Hydroxyl
O	Atomic Oxygen
O2	Superoxide
D1	Dilution 1
D2	Dilution 2
D3	Dilution 3
D4	Dilution 4

ATC	Automatic Temperature Compensation
LCD	Liquid Crystal Display
S	Siemens
PPM	Parts Per Million
g/L	Grams/Liter
V	Volts
NaCl 0.9	Isotonic Saline
Ri-Lac	Ringer's Lactate
1/1 E	Jonosteril
PTFE	Polytetrafluoroethylene
PLA	Polylactic Acid
UV	Ultra Violet
LED	Light Emitting Diode

Abstract

The evolution and application of plasma-based medicine are continually advancing, with a specific focus on the precise and efficient detection of reactive species, such as RONS, in PAL.

An exhaustive exploration of sensors is undertaken, beginning with the implementation and initial evaluation of calibration sensors, setting a solid foundation for future measurements. Through meticulous research, the most suitable sensor for RONS detection is selected.

A significant achievement of this study is the design of a 3D model for a specialized PAL flow control system, optimizing data capture and analysis. This system is precisely materialized using CNC machine tools.

Finally, measurements are conducted using the designed system in conjunction with the chosen sensor. Collectively, these efforts represent a notable advancement in plasma-based medicine, providing tools and techniques for future developments in this field.

Keywords: plasma-based medicine, reactive species, RONS, PAL, sensors, 3D model design, CNC machine tools, measurements;

Acknowledgements

I would like to thank Jan Mitrovics for having relied on me since the first moment and giving me the opportunity to do an internship in his company in Germany. Furthermore, I extend my appreciation to my colleagues at work and to the company BlueLab for providing the necessary materials for conducting experiments, as well as for their valuable contributions of ideas and solutions.

I would especially like to thank David Girbau for supporting and helping me both as my double degree coordinator during the last five years and as my tutor in this project, for his guidelines and corrections.

Finally, to my family and friends, who supported me during the whole process from a distance. In addition, I want to give special thanks to my boyfriend, who was a fundamental pillar during the six months that my Erasmus experience lasted.

Contents

1 Introduction **11**

1.1 Company 12

1.2 EndoPAL project 15

1.2.1 Plasma Activated Water 18

1.3 Objectives 20

1.4 Document organization 20

2 Sensors **23**

2.1 Reference Sensors 23

2.1.1 Multi-Parameter Tester 23

2.1.2 Arduino-Compatible TDS Sensor 25

2.2 Conductivity Sensor 29

2.2.1 Platinum Electrodes 30

3 Chamber **33**

3.1 Design 33

3.2 Manufacture 36

3.3 Sensor installation 39

4 Measurements collection **41**

4.1 Measurement System 41

4.2 Data collection 43

4.3 Data validation 46

4.4 Data discussion 48

5 Conclusions **51**

References **53**

A Appendix 1. Additional figures **55**

1 Introduction

The ability to measure accurately is essential to scientific and technological advancement since ancient times. Whether it is determining the position of the stars for navigation, measuring the amount of ingredients in a recipe, or determining the concentration of a drug in the blood, measurements play a crucial role in almost every aspect of life.

Nowadays, with the rapid progress of technology and science, sensors are become central in ensuring the measurements are correct. Sensors play an essential role in capturing and translating real-world parameters. At their core, sensors are devices capable of sensing, or responding, to a specific parameter and converting this information into a usable signal output, working according to a predetermined set of rules [1]. In more technical terms, a sensor acts as a transducer. Its primary function is to measure a variable of interest, which can be mechanical, thermal, magnetic, electrical, optical, among others, and then transform this data into another, more easily measurable variable, usually of an electrical nature [2].

When categorizing sensors based on their output, they broadly fall into two main types. Analog transducers, which provide a continuous analog signal, and digital transducers that yield a digital output. This digital signal can either be in the form of a set of parallel status bits or a series of countable pulses.

However, for a sensor to be genuinely valuable as a measuring tool, there's a crucial step involved: calibration. This process ensures that there's a well-defined relationship between the variable being measured and the converted output signal produced by the sensor. Furthermore, when it comes to selecting the right sensor for a task, several considerations come into play. Factors like the shape of the sensor's housing, its operating distance, and specific electrical data and connection methods are essential to ensure optimal performance and accuracy [2].

In the realm of medicine, where accurate measurement is fundamental from diagnosis to treatment [1], sensors, known as biomedical sensors, take on a paramount significance. They ensure the precise capture of measurements in a manner that's safe for the patient [3]. As the medical field advances toward more individualized and precise practices, the demand for these reliable sensors surges. Biomedical sensors are specialized electronic devices that transduce or convert biomedical signals into more easily measurable electric signals. Their role is crucial in enabling real-time monitoring and tailored interventions for individual patients, and they are integral components in various medical diagnostic instruments [4]. From there, biomedical instrumentation refers to the ensemble of tools and equipment specifically designed to acquire, process, and interpret the signals obtained from these sensors. This instrumentation facilitates better patient care by providing accurate and timely data, assisting clinicians in making informed decisions and improving therapeutic outcomes.

Many features typical of general instrumentation systems are also present in biomedical instrumentation systems. A standard medical instrumentation setup consists of essential elements such as the measurand, the sensor or transducer, the signal conditioner, and the display system [5]. As we can see in the diagram of *Figure 1*, what reaches the sensor is a variation of a certain magnitude. This change passes through the sensor to transform it into an electrical signal, and then it is treated so that this signal can be processed and we can get information from it [2].

Having outlined the essential elements of a biomedical instrumentation system, it is clear

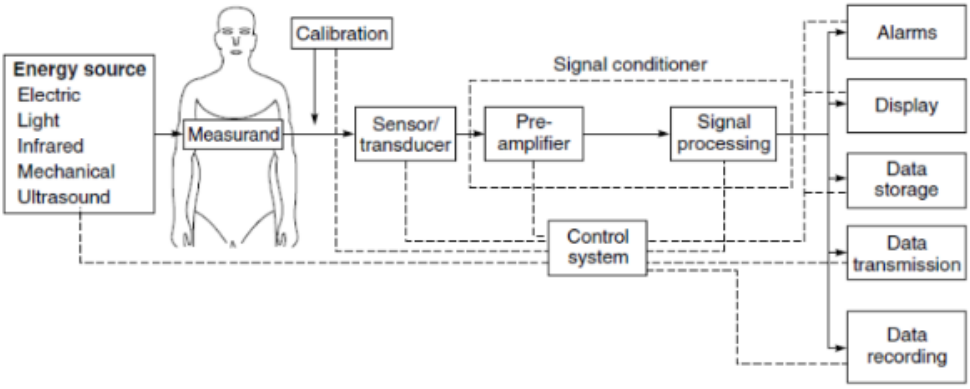

Figure 1. Block Diagram of a Medical Instrumentation System [5]

that the precise choice and application of sensors are paramount. Considering the three main types of sensors[1], the thesis focuses on the monitoring and control of reactive species in a PAL. When administered through an endoscope during surgical interventions, the goal is to reduce postoperative adhesions. For this purpose, it is deploy a chemical sensor capable of accurately detecting chemical alterations.

1.1 Company

JLM Innovation GmbH is a technology company based in Tübingen, Germany. It is established by Jan Mitrovics, who serves as the CEO, in 2004. The company possesses technological expertise encompassing various hardware and software aspects related to data acquisition and subsequent analysis. They offer software and hardware platforms, as shown in *Table 1*, catering to smart sensors, sensor systems, and sensor networks designed for gas sensing in both commercial and academic Research and Development contexts. These platforms incorporate advanced algorithms for tasks such as feature extraction, pre-processing, and pattern recognition. Additionally, there is support for multiple platforms[2], along with software libraries for programming languages such as C, C, Java, Python, Delphi, LabVIEW, among others.

Products	**Explanation**
ModularBA/miniBABreath	Analysis systems for clinical research
MiniMOX /MOXbox	Multi MOX sensor platforms
MOXstick/GIGAstick	USB interface for resistive gas sensors
CAPmeter	USB interface for capacitive sensors
JLMQ/FQ4 QMB and SAW	Sensor platforms
ZNet/ZigSens/Snet	Wireless sensor networks

Table 1. The products and platforms for research and development

For more than fifteen years, JLM Innovation GmbH is engaged in the field of chemical sensing. This implies their continuous efforts to devise methodologies for detecting a wide

[1]Physical, chemical, and biological quantity sensors
[2]Windows 10, MacOS, Linux, Android, iOS, Embedded/MCU

range of chemicals across various domains such as air quality, health, automotive, food, explosives, and toxic substances. To achieve this, they are harnessed an assortment of technologies, including MOX, MEMS, nanotechnology, and diverse sensing techniques. Additionally, they extend services aimed at facilitating the creation of tailored solutions. This encompasses tasks like sensor application development, sensor selection and enhancement, electronics and hardware design, firmware development, algorithm creation, and frontend software design. Within their facilities, particularly their laboratory, they offer access to an extensive array of technology components, which proves instrumental in the development and enhancement of projects.

The company collaborates with a multitude of partners worldwide, including universities and companies, engaging in extensive exchange of ideas and solutions through various prominent research endeavors:

- Participation in European and national funding initiatives such as Horizon 2020 and BMBF
- Pioneering the creation of innovative chemical sensor technologies targeting medical and safety applications
- Conducting clinical studies in collaboration with partners across Europe, South America, and Asia
- Innovating advanced algorithms and operational modes to address drift and cross-interference compensation in chemical sensor arrays
- Developing instrumentation geared towards medical diagnosis
- Designing sensor networks and cloud platforms for distributed sensing
- Focusing on miniaturization, integration, cost reduction, and power efficiency enhancements for smart sensors

They have also been involved in some research projects:

- LCaos (04/2011 – 03/2015)
- Volgacore (07/2014 – 06/2017)
- SniffPhone (02/2015 – 02/2019)
- TropSense (02/2015 – 01/2019)
- Sensoft (01/2019 – 12/2023)
- 3D-PAKtex (01/2020 – 06/2023)
- EndoPAL-i (10/2022 – 09/2024)

Among these research projects in which the company is involved, the EndoPAL project stands out. One of the main results up to now of this project is the design and program of a PCB (see in *Figure 2*) that can detect the presence of species by measuring the impedance, also know as resistance, of the water.

Beyond this initial task, the development of an internal sensing process in the project is assigned to me. This involves selecting the most suitable sensor, integrating it into the PCB and ensuring that it reliably measured the impedance in a solution. The collection of this data over time makes monitoring PAL endoscopic application during surgery possible. Specifically, invasive abdominal procedures often lead to postoperative adhesions, pathological bonds that form between surfaces within the body cavity. Such bonds can directly or indirectly

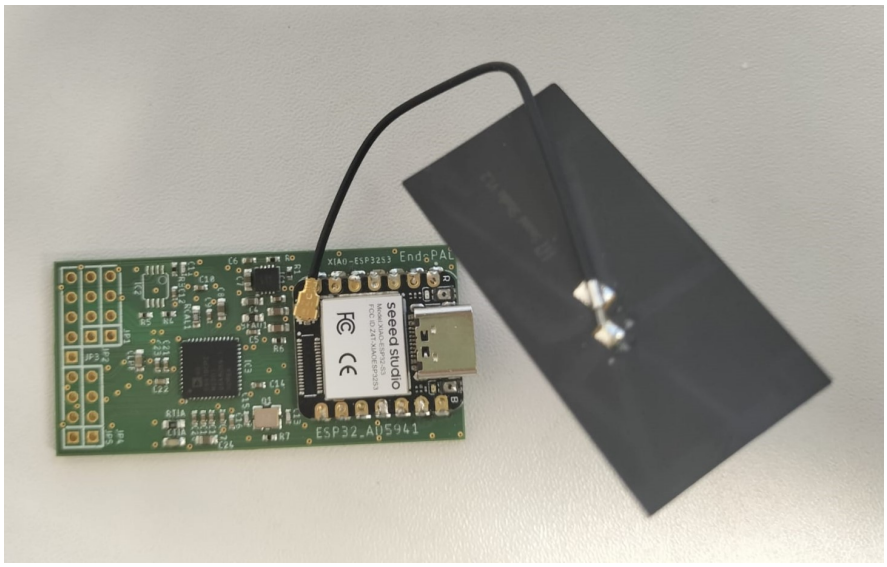

Figure 2. PCB populated with an antenna

cause complications, including chronic pain, organ dysfunction, and can increase the need for multiple operations.

In 2018, around 2.6 million abdominal surgeries, both open and minimally invasive, are performed in Germany, reflecting a growing trend worldwide. In Germany alone, it is estimated that there are 1.75 - 2.4 million new cases each year. Therefore, there is a significant clinical demand for effective prevention against adhesions that can be consistently incorporated into surgical procedures. PAL can modulate the proliferation and protein synthesis of healthy connective tissue cells, such as mesothelial cells and fibroblasts, in a dose-dependent manner. This capability can help prevent the overproduction of extracellular matrices (see in *Figure 3*), which are the primary cause of postoperative adhesions [6].

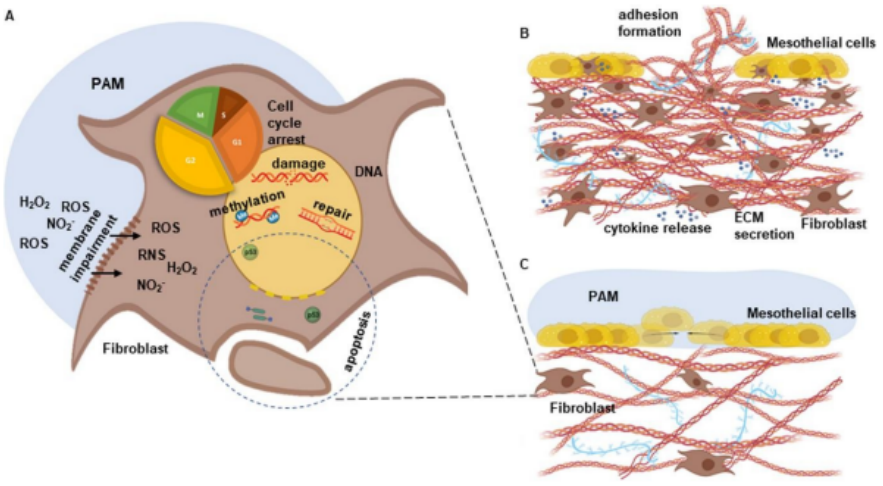

Figure 3. Biologic schematic representation with (A) different reactive species concentrations dissolved in the PAM that induce different cell type-specific responses inside a cell, and (B) a pathological cell response as a result of peritoneal injury. (C) After the treatment, it is able to observe a cell type-specific inhibition of proliferation and protein secretion in fibroblasts with unhindered re-epithelialization

Considering the statistics and potential complications arising from postoperative adhesions, the advances made in the EndoPAL project, in particular the integration and optimization of detection technology, are critical to ensure accurate measurement and real-time application of

PAL during surgical procedures.

1.2 EndoPAL project

EndoPAL project aims to develop a compact system for generation and endoscopic application of PALs for the prophylaxis of postoperative adhesions. The essence of this initiative lies in harnessing the unique properties of plasma in medicine.

The matter has always been classified into three states: solid, liquid and gas. However, in 1928, Langmuir introduces plasma as the fourth fundamental state of matter [7], the most common state of matter in the universe, found in stars, including the sun, and in interstellar and intergalactic spaces. From lighting up neon signs and plasma TVs to being integral in material processing, the breakthrough in understanding plasma's capabilities comes when it begins to be utilized in medical applications, underscoring its remarkable versatility.

Initially, the usefulness of plasma in medicine is limited by its high temperature, often exceeding several thousand degrees, assuming a risk of thermal damage to living cells [8]. Those high temperatures result from frequent collisions between electrons and heavy particles, bringing all particles towards thermal equilibrium. However, there are cases where plasma discharges occur quickly, leading to a state where electrons and heavy particles exist in thermal disequilibrium. Here, the temperature of the heavier particles is significantly lower than that of the electrons. This is known as CAP [9], where the temperature of the heavy particles ranges between 25°C and 45°C. Due to this feature, CAP does not cause thermal damage when interacting with patients' tissues.

After determining the specific type of plasma used for medical applications, it's essential to understand its generation for the project's needs. A DC discharge, see in *Figure 4*, is a type of gas discharge, the easiest way of generating plasma. It occurs when a constant or direct electrical current is applied to a neutral gas within a certain pressure range, causing the gas to ionize and conduct electricity [10][11]. In ionization, the energy level becomes substantial enough for an electron to overcome the electrostatic potential barrier, the electron gets ejected from the atoms or molecules of the gas, and it results in the formation of a free electron and a positively charged ion[3] [8]. The sustained flow of DC ensures that the gas remains ionized for a prolonged period, making it suitable for medical applications.

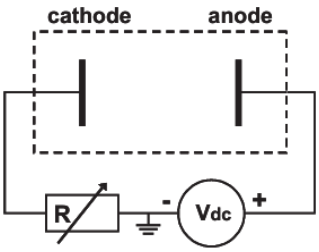

Figure 4. Schematic diagram of a DC discharge between parallel plate electrodes, where the flow of electric discharge is constant in direction, from the positive to the negative terminal [10]

The main sources capable of generating plasma by means of a DC discharge are the plasma jet device and the DBD device. As shown in *Figure 5*, both devices share similar physical principles, components, and materials. In these two devices, a violet plasma is generated

[3]There are numerous particles interacting in gas discharges, neutral and both positively and negatively charged particles, mainly electrons, ions, neutral atoms and molecules

between an anode and a cathode. Simultaneously, the anode or cathode is covered with a layer of dielectric materials such as quartz. However, both devices differ in how they operate [8]. It is possible to see the differences in *Table 2*.

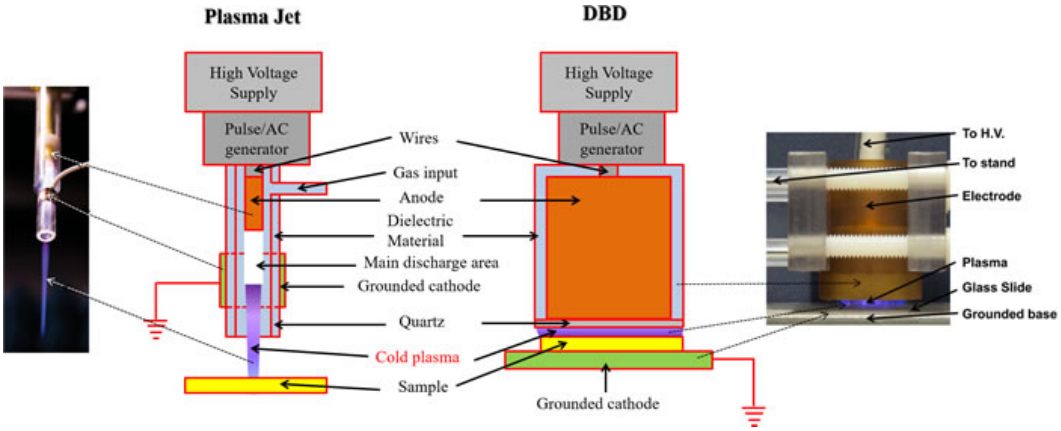

Figure 5. The plasma jet and the DBD are two main CAP devices used in plasma medicine. The same components in both devices are drawn with the same colors

Plasma Jet	**DBD**
It needs a carrier gas such as helium or argon to sustain the formation of CAP. Due to the continuous flow of the carrier gas, a CAP jet is formed	It can generate the plasma directly in air, a short but wide plasma
The sample is simply treated by the plasma jet	The is not generated if the sample is not adequately close to the second electrode
It may be more suitable to gently treat a small area of a sample	It may be more suitable for more intense treatment on a large sample area

Table 2. Comparative table of two CAP sources

If the aforementioned plasma interacts with liquids, it produces powerful activated solutions that can reach areas challenging for direct plasma application [9].

PAL results from the exposure of liquids to a plasma discharge either directly, where the discharge happens inside or in contact with the liquid or indirectly through exposure to the plasma afterglow[4] [12]. Its activation promotes the physicochemical reactions that create reactive species with unpaired electrons[5], such as RONS [13]. Generally, as can be seen in *Figure 6*, the species are first produced in an atmospheric pressure plasma in the gas phase. A fraction of these species is then transported to the plasma–liquid interface, traversing the interface and subsequently reacting with the molecules of the liquid medium. Importantly, gas-phase generated radicals and molecules have a significant impact on the formation of numerous reactive species, for example the chemical radicals H2O2, NO2, NO3, and ONOO-, in aqueous solutions [14] [15].

Parameters such as the type of plasma generation gas, plasma power, reactor type, and molecular interactions at the plasma-liquid interface can influence the composition, quantity,

[4]See the difference in *Figure 49*, Appendix 1

[5]They can easily interact with other elements, participating in many chemical reactions

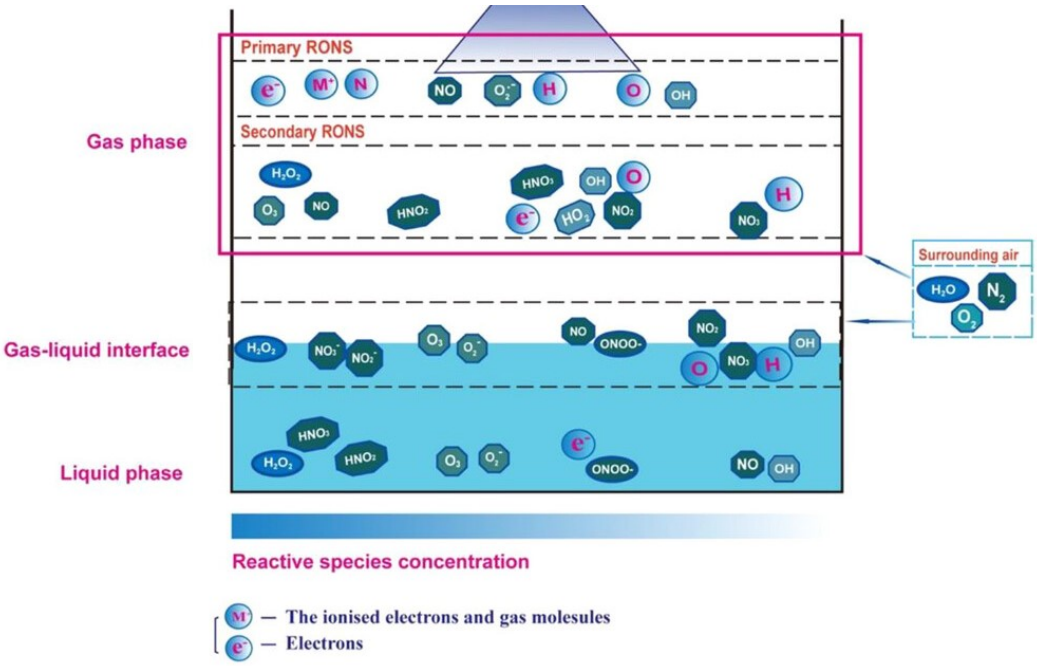

Figure 6. Formation of reactive species in plasma activated liquid solutions [16]

and lifetime of RONS (as can be seen in *Table 3*), as well as change the acidity of the activated solution [13].

Specie	Estimated half-life
$OH\bullet$	ns
$NO_2\bullet$	µs
O_2-	ms
$ONOO-$	ms
$NO\bullet$	1 - 10 s
$1O_2$	10 s
H_2O_2	minutes
NO_2-	minutes
NO_3-	minutes

Table 3. RONS estimated half-life

The presence of reactive species in PALs is influenced by the intrinsic properties of the liquids themselves[6] and can be measured indirectly through physicochemical parameters such as pH, EC, TDS, and salinity, among others [12] [17].

- *pH* is the measure of the hydrogen ion concentration of a solution
- *EC* indicates the ability of an aqueous solution to conduct electricity, which depends on the types of ions, their concentrations, and the solution temperature

[6]Its conductivity, chemical composition, viscosity, surface tension and temperature

- *TDS* is a measure of the dissolved combined content of all inorganic and organic substances present in a liquid in molecular, ionized, or microgranular suspended form
- *Salinity* is the measure of the concentration of dissolved salts in a solution

One of the most researched and applied forms of PAL is PAW. It typically refers to the activation of DI water by plasma, thus impregnating water with reactive species, altering its properties and making it suitable for medical applications.

1.2.1 Plasma Activated Water

Unique transfer of chemical reactivity and energy from gaseous plasmas to water takes place in the absence of any other chemicals, but results in a product with a notable transient broad-spectrum biological activity, referred to as PAW [14]. In most cases, as shown in figure *Figure 7*, the different plasma treatments lead to an acidification of the water, the pH decreases, and it starts to conduct better the electricity, the EC increases [18].

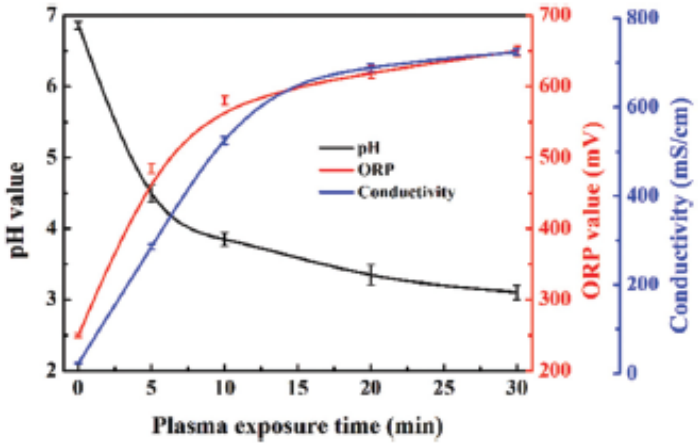

Figure 7. Physicochemical properties of PAW after plasma exposure at different times [15]

The EC serves as a vital marker for the presence of reactive ions in water. After undergoing air plasma activation for 30 minutes, the EC of PAW surges from 24 to 724 μS cm^{-1}. This sharp increase signifies the creation of multiple active species due to interactions between plasma and water molecules at the gas-liquid interface (see in *Figure 8*). Additionally, data implies a notable association between the total concentration of RONS in PAW and the duration of plasma activation, reinforcing the idea that reactive species can build up in PAW. A noticeable decline in water pH is observed post-plasma exposure, which can be linked to the generation of nitrous and nitrate acids when NOx species react with water molecules [15].

In PAW, reactive species have varying lifetimes, either short-lived or long-lived. Among the short-lived species, 1O2, -OH, O and O2 stand out. On the contrary, as shown in *Figure 9*, among the long-lived species, H2O2 stands out, which is easy to detect due to its stability [18], in addition to other secondary species formed in the liquid, such as NO2- and NO3- [14] [15].

To understand the interactions of the species, and their potential benefits for the project, four different PAW solutions are prepared mixing concentrated PAW at pH 1.84 and DI water at pH 5.8[7], as shown in *Table 4*. Both are control solutions. The choice of DI water as the

[7]See them in *Figure 50*, Appendix 1

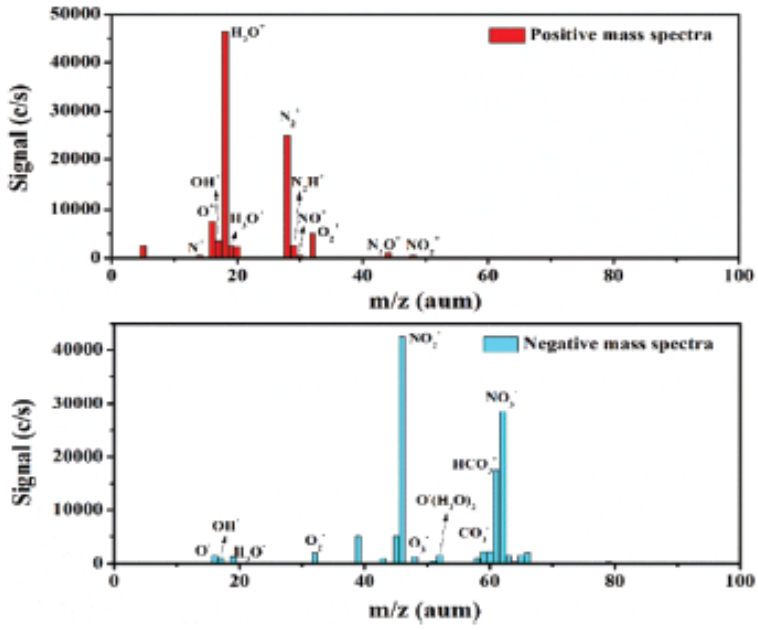

Figure 8. Time-averaged mass spectra of plasma generated negative and positive ions by energetic electron ionization of water molecules at gas–liquid interface [15]

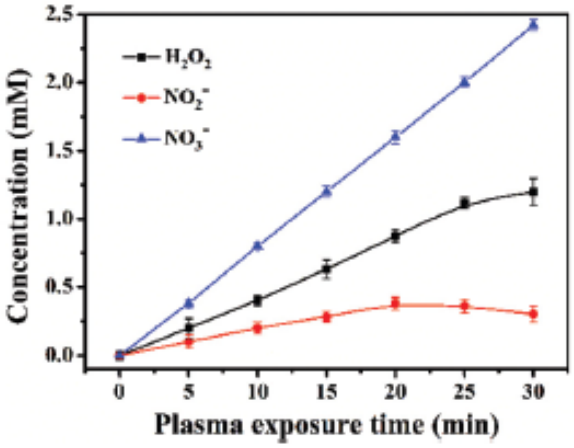

Figure 9. The concentrations of H2O2, NO2 − and NO3 − in PAW with different plasma exposure times [15]

control solution provides a baseline, due to its inherent lack of ions, ensuring the absence of possible conductive interferences.

D1	5 mL PAW + 45 mL DI water
D2	5 mL D1 + 45 mL DI water
D3	5 mL D2 + 45 mL DI water
D4	5 mL D3 + 45 mL DI water

Table 4. PAW solutions. Each dilution is obtained by mixing 5 mL of the previous dilution with 45 mL of DI water

The preparation of these PAW solutions, together with the use of appropriate control solutions, lays the foundation for rigorous experimentation and analysis.

1.3 Objectives

In this thesis I focus on the development of an internal sensing process in the EndoPAL project. This involves selecting the most suitable sensor, integrating it on the PCB and ensuring with calibration sensors that it reliably measures the resistance in a PAL solution, value that can be influenced by the number of dissolved species. The sensor is integrated into a specifically designed and manufactured chamber for the measurement process, in which the solution is passed through a closed system for a period of time.

The main objectives are listed below:

- Calibration and initial evaluation of some reference sensors. These sensors serve as a baseline for comparison against the chosen optimal sensor. The reference sensors are likely to be established sensor models that are already known for their accuracy and reliability in measuring certain properties related to the species in a solution, including pH, conductivity and TDS. Establish a benchmark for evaluating the performance of the optimal sensor later in the project
- Research and selection of the optimal sensor for species detection. The research process involves evaluating various sensor options based on factors such as sensitivity, specificity, cost, and compatibility with the EndoPAL project's requirements. Once the optimal sensor is selected, it plays a critical role in accurately detecting species in the solution
- Design of a 3D model of a special chamber for PAL flow control in a closed system. The shape, dimensions and internal characteristics of the chamber are critical for effective fluid flow control. Fluid dynamics simulations are necessary to optimize the internal structure of the chamber, ensuring uniform flow distribution, minimum turbulence and adequate residence time of the solution inside the chamber
- Manufacture of the chamber using different tools. This process involves using various technologies, such as additive manufacturing (3D printing), CNC machining, or other fabrication methods. The goal is to accurately reproduce the designed chamber and ensure its functionality as intended
- Perform system measurements with the optimal sensor. Measurements are made using a configured system. The solution containing species is passed through the closed loop, a pump, a glass container and the chamber, and sensor readings are recorded. This step is intended to validate the performance of the system to accurately detect and quantify the levels of species
- Analyze the accuracy of the measurements. The collected data is compared to known standards or reference measurements to assess the accuracy of the optimal sensor and the overall system. This analysis highlights the system's ability to reliably measure resistance in a PAL solution, thus validating its effectiveness for species detection

1.4 Document organization

The thesis begins with an explanation of the fundamental principles of sensors and measurement systems in general, examines the experimental framework in which the research is carried out and establishes the objectives to be achieved.

The second chapter presents a description of the sensors used, two reference sensors and a conductivity sensor, including how to calibrate them and subsequent measurements.

The third chapter presents the designed and manufactured chamber. This serves as a fundamental component to house the conductivity sensor, integrating it perfectly into the experimental setup.

The final chapter begins with the configuration of the measurement system, continues with the data collection, the data validation and, finally, the data analysis.

Finally, the references section presents a comprehensive catalog of all materials and references used throughout the research, affirming that the research is based on solid academic foundations.

2 Sensors

2.1 Reference Sensors

Ensuring accurate and consistent measurements in PAW research is paramount, especially considering their complex behavior when characterizing the physicochemical properties. To ensure high-precision measurements and minimize errors [19], it's essential to use sensors which act as a reference when comparing readings.

2.1.1 Multi-Parameter Tester

The PC60 Premium multiparameter tester, observe in *Figure 10*, is recognized for its ability to measure multiple parameters with its electrode. Among the parameters that can be measured in aqueous solutions, where the main solvent is water, include pH, conductivity, TDS, salinity, and temperature[1]. Its ATC feature, operational within a 0 to 50°C range, ensures the measurements remain consistent despite temperature variations [20]. Moreover, integral to its design, the tester comes with a default TDS factor set at 0.71[2]. This factor, adjustable within a 0.40 to 1.00 range depending on the solution's specifics, is crucial for converting conductivity readings to TDS values with *Equation 1*, where k is the TDS factor and EC the electric conductivity. [21].

Figure 10. PC60 Premium Multi-Parameter Tester Kit

$$TDS(ppm) = k \times EC(\mu S/cm) \tag{1}$$

To ensure that the multi-parameter tester operates at its peak performance, collecting correct and accurate readings, it is necessary to calibrate it with conductivity and pH buffers[3] beforehand.

Calibration begins by immersing the probe in DI water and then drying it. The probe is then immersed in the calibration buffer solution and gently agitated. It is important to allow the probe to stand in the solution, waiting for a stable reading. As soon as the LCD display

[1] Observe the technical specifications in *Figure 51*, Appendix 1
[2] Observe it in the multi-parameter tester in *Figure 52*, Appendix 1
[3] See the four calibration buffer solutions in *Figure 53*, Appendix 1

steadily shows the stability icon, a short press of the key completes the calibration [21] [22]. As can be seen in *Figure 11*, the calibration is correctly done.

(a) Conductivity 1413 µS/cm (b) Conductivity 12.88 µS/cm (c) pH 7 (d) pH 4

Figure 11. Conductivity and pH calibrations, respectively

After successfully calibrating the device, the parameters of some PAW solutions[4] are measured at an ambient temperature of 27ºC (observe in *Table 5*). To measure, the probe is immersed, gently agitated[5] and stands still inside the solution until a stable reading is reached [21]. For the temperature measurement, the probe does not need to be immersed in the solution, as the temperature is collected at the same time with the other parameters.

	PAW	D1	D2	D3	D4	DI water
Conductivity [μS/cm]	1198	630	83	8	1	0
pH	1.84	2.94	4.03	5.49	5.61	5.80
TDS [ppm]	586	302	39	4.40	0.30	0.00
Salinity [g/L]	0.53	0.30	0.02	0.00	0.00	0.00
Temperature [ºC][6]	32.3	31.9	31.9	31.7	31.5	27.7

Table 5. Measurement results with PC60 Premium Multi-Parameter Tester

The data presented in *Table 5* shows a decreasing trend in conductivity, TDS and salinity as the PAW is more diluted. In addition, while the first two dilutions, D1 and D2, show a more acidic pH, respectively, and detectable salinity, the remaining two dilutions tend toward neutrality and have minimal or undetectable salinity. On another hand, it is notable that DI water, which is the basis for these dilutions, exhibits a lower temperature. This can be attributed to the absence of ions in DI water. The presence of ions in a solution can influence its thermal properties, and, when mixing DI water with PAW, ions are introduced, which could result in a slightly elevated temperature compared to pure DI water.

[4]Observe the four types of dilutions prepared in *Figure 50*, Appendix 1
[5]Important to be able to measure all species
[6]It is the average temperature of the measurements of the other parameters

2.1.2 Arduino-Compatible TDS Sensor

The Arduino-compatible TDS sensor launched by CQRobot[7] is recognized for its ability to measure TDS value of water after connecting to an arduino controller. A TDS value is indicative of the milligrams of dissolved solids present in a liter of water. The higher this value, the more impurities can be inferred in the water, positioning TDS as a key indicator of water purity. The integration of the TDS sensor with the Arduino platform, observed in *Figure 12*, allows for direct and efficient sensor readings, which can be seamlessly interpreted in the Arduino environment. These readings in real time, especially with water quality metrics, can pose challenges in terms of data fluctuation and environmental interference. However, CQRobot provides robust basic libraries and preliminary code scripts optimized for accuracy and stability in such applications.

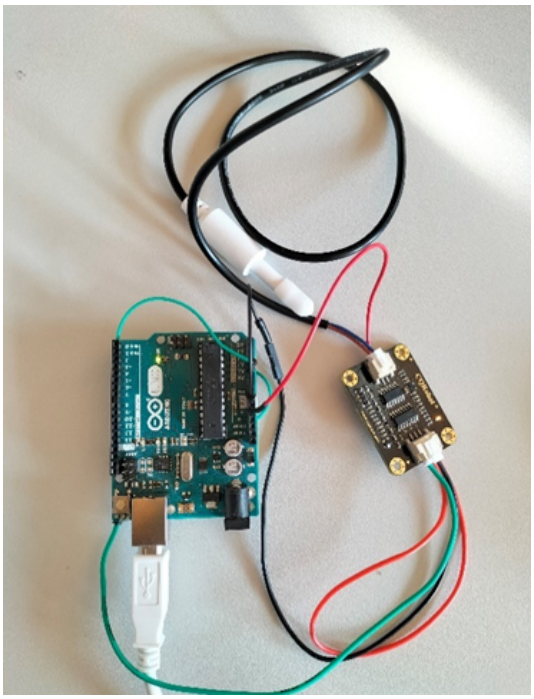

Figure 12. TDS meter sensor compatible with Raspberry Pi/Arduino board by CQRobot Ocean

Observe in *Code 1*, the part of the code that is of most interest for collecting measurements with the sensor. This code, a CQRobot resource, is used and tested within the Visual Studio (VS) Code Editor environment.

```
//It calculates a temperature compensation coefficient and
//calculates the TDS value taking that value into account
 float compensationCoefficient = 1.0 + 0.02 * (temperature - 25.0);
 //Temperature compensation
 float compensationVolatge = averageVoltage / compensationCoefficient;
 //Convert voltage value to tds value
 tdsValue = (133.42 * compensationVolatge * compensationVolatge *
compensationVolatge - 255.86 * compensationVolatge *
 compensationVolatge + 857.39 * compensationVolatge) * 0.5;
```

Code 1. Part of the code in [23]

[7]Observe the technical specifications in *Figure 54*, Appendix 1

In the given Arduino program, multiple samples are taken from the sensor reading, and then a median filter is applied to reduce noise and obtain a more stable value. This value is adjusted for temperature, which is pre-set to 19.5°C in this code, as the TDS reading can vary with temperature. Once the reading is temperature compensated, the actual TDS value in ppm is calculated using a polynomial equation.

Calibration must be performed beforehand to obtain accurate TDS values. For the calibration of the TDS sensor, it is used the medical solutions shown in *Figure 13*, and the PC60 premium multi-parameter tester[8], as shown in *Figure 14*, *Figure 15* and *Figure 16*.

(a) NaCl 0.9 solution (b) Ri-Lac solution (c) 1/1 E solution

Figure 13. Three different medical solutions

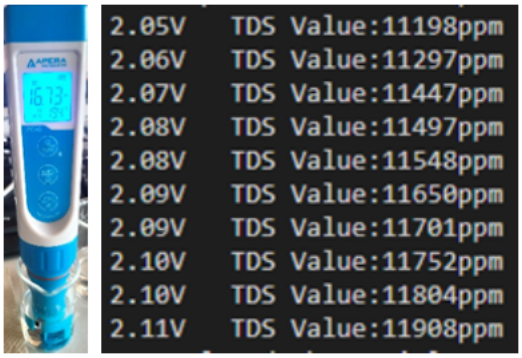

Figure 14. Conductivity measurement, and voltage and TDS measurements, respectively, in NaCl 0.9 solution

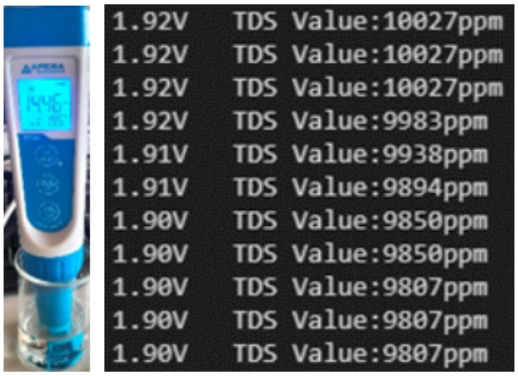

Figure 15. Conductivity measurement, and voltage and TDS measurements, respectively, in Ri-Lac solution

[8]Previously proven to be a reliable measurement device

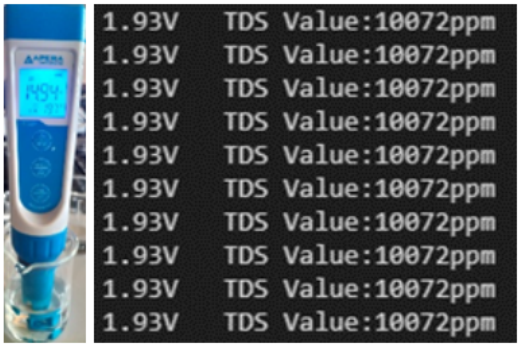

Figure 16. Conductivity measurement, and voltage and TDS measurements, respectively, in 1/1 E solution

In conclusion, the TDS sensor is correctly calibrated with the multi-parameter tester. It can be seen in *Table 6* that when measuring the solutions in *Figure 13* with the sensors, the TDS values are very similar in both sensors.

		NaCl0.9 solution	**Ri-Lac solution**	**1/1E solution**
Multi-parameter tester	**Conductivity [μS/cm]**	16730	14460	14940
	TDS [ppm][9]	11878	10266	10607
TDS sensor	**Voltage [V]**	2.08	1.91	1.93
	TDS [ppm]	11500	9900	10072

Table 6. Conductivity, TDS values and voltage of multi-parameter tester and TDS sensor

To ensure accurate measurements with the TDS sensor, apart from pre-calibration, it is important to follow the protocol and care of the instrument:

- Adequate agitation is required to counteract possible concentration gradients in the analyte
- The placement of the probe is critical; ensuring central immersion avoids boundary effects that can introduce systematic drifts in readings
- Rinsing the electrode after measurement is paramount to mitigate potential ion build-up and contamination. An immaculate, residue-free electrode surface ensures optimal electrode conductance and response time

As shown in *Table 7*, the electrode is immersed to measure the TDS parameter and voltage[10] in the solutions[11].

[9]Calculated with *Equation 1*. TDSNaCl = 0.71 ×16730 μS/cm = 11878 ppm, TDSRiLac = 0.71 ×14460 μS/cm = 10266 ppm, TDS1/1E = 0.71 ×14940 μS/cm = 10607 ppm

[10]Observe the set-up to measure with the multimeter in *Figure 55* and the comprobation measurements in *Figure 56*, Appendix 1

[11]Observe the four types of dilutions prepared in *Figure 50*, Appendix 1

		PAW	D1	D2	D3	D4	DI water
TDS [ppm]	**Arduino**	557	290	32	0	0	0
Voltage [V]	**Arduino**	1.42	0.70	0.07	0.00	0.00	0.00
	Multimeter	1.440	0.722	0.080	0.015	0.010	0.00

Table 7. Measurement results with Arduino-compatible TDS sensor

In the conducted experiments, the data in *Table 7* consistently aligns with the multi-parameter tester results. Both the Arduino-compatible TDS sensor and the multi-parameter tester exhibit a decreasing TDS pattern as PAW becomes more diluted. These results validate the general trend of decreasing ion concentration in dilute solutions. The small differences in numerical values, with the TDS sensor values being slightly smaller, may be due to sensor calibration, sensor accuracy or sensor temperature compensation. The temperature compensation coefficient might be different in both sensors, meanwhile in the multi-parameter tester is used the factor in *Figure 17*, in the TDS sensor is used the formula in *Code 2*. The code performs calculations to adjust an average voltage as a function of temperature. This is accomplished by calculating an offset coefficient based on the difference between the actual temperature and a reference temperature. The average voltage is then divided by this compensation coefficient to obtain a compensated voltage that reflects the influence of temperature on the voltage measurement.

P4	Temperature compensation factor	0.00 - 4.00%	2.00%

Figure 17. Default factor of the multi-parameter tester [21]

```
float compensationCoefficient = 1.0 + 0.02 * (temperature - 25.0);
float compensationVoltage = averageVoltage / compensationCoefficient;
```

Code 2. Temperature compensation coefficient used in voltage compensation formula, TDS sensor

After validating both sensors and confirming their accurate and consistent measurement performance, the next step involves determining the *k* factor of the TDS sensor. This factor is essential to convert TDS readings into conductivity measurements, as the TDS sensor is not able to measure them. This conversion enables a meaningful comparison with the readings from the multi-parameter tester. By considering the data collected from both sensors, the *k* factor is 0.47, a value that aligns with the observations presented in *Table 8*.

		PAW	D1	D2
Multi-parameter tester	**TDS [ppm]**	586	302	39
	Conductivity [μS/cm]	1198	630	53
TDS sensor	**TDS [ppm]**	557	290	32
	Conductivity [μS/cm][12]	*1185*	*617*	*68*

Table 8. Comparison of TDS and conductivity results with both sensors to derive the *k* factor of the TDS sensor

It is now possible to validate the conductivity sensor by comparing it with reliable standard sensors.

2.2 Conductivity Sensor

For monitoring PAW over time, the sensor shown in *Figure 18*, is used. Its technical specifications are detailed in *Figure 57*.

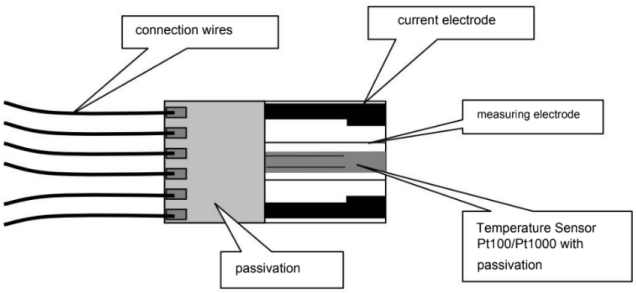

(a) Schematic layout

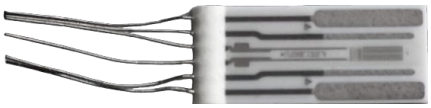

(b) Dimensions: 7 mm x 14 mm

Figure 18. The sensor is divided in two zones, the electrode zone and the passive zone. The passive zone has a layer on the sensor's surface to prevent it from reacting with the environment

The sensor measures the resistance (R), in Ohms (Ω), relates to the conductance (G), in Siemens (S), by means of *Equation 2*, in the context of DC. While resistance opposes the flow of electric current in a material or component, conductance is the ease with which a material or component allows electric current to flow.

$$G = \frac{1}{R} \tag{2}$$

[12] Calculated with *Equation 1*. CondPAW = $\frac{557}{0.47} \approx 1185$ μS/cm, CondD1 = $\frac{290}{0.47} \approx 617$ μS/cm, CondD2 = $\frac{32}{0.47} \approx 68$ μS/cm

While the conductivity sensor allows only the calculation of the conductance of a solution, the reference sensors focus on the conductivity of the solution. Conductance and conductivity are linked by *Equation 3*, wherein A represents the cross-sectional area through which the current flows, and L signifies the length of the material along which the current travels. However, it is not possible to obtain this surface data from the measurement system. The current flow circulates over an unknown area and length in the experiment, as can be seen in the measurement system set up in Chapter 4. Measurements collection. Therefore, the conductance measurements are compared with the conductivity measurements, electrical properties of a solution

$$G = \sigma \cdot \frac{A}{L} \tag{3}$$

Both electrical properties are essential to deduce ionic concentrations [17], as they provide insight into the molecular composition of the solution. The principle underlying this measurement is based on the behavior of ions under voltage, acting as charge carriers, they facilitate current flow. The sensor level of the conductance is determined by two temperature-sensitive factors, the ion concentration and the mobility of these ions. To fine-tune the accuracy of these observations, a specific temperature sensor, protected against mechanical stress with a glass passivation layer, is meticulously placed at the same location as the measurement [24]. The explained is visually represented in *Figure 19*, where the relationship between conductivity and temperature during plasma treatment is shown.

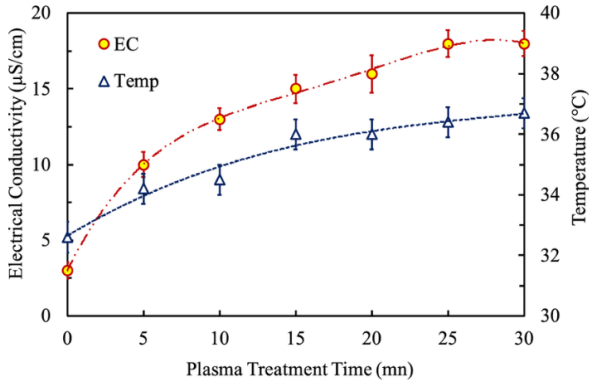

Figure 19. Concentration of NO2, NO3, and H2O2 in water as function of plasma treatment time [25]

To perform conductance measurements in PAW with the sensor, it is necessary to take into account the types of electrodes that are used, so that they do not interfere with the measurements.

2.2.1 Platinum Electrodes

The optimal performance of the sensor depends on its electrodes. The electrodes are metals whose surface serves as the primary interface with the solution [26], facilitating the site of oxidation-reduction reactions. They assist in the transport of electrons, generating an electrical charge. Depending on its role in the electrical process, an electrode can function as either an anode or a cathode. As shown in *Figure 20*, two types of electrodes are used, current and measuring electrodes. While the current electrodes supply an alternating current (AC) to the solution, the measuring electrodes detect the resulting voltage. Knowing the

current passing through the solution and the detected voltage, in *Equation 4*, the resistance and conductance of the solution can be obtained.

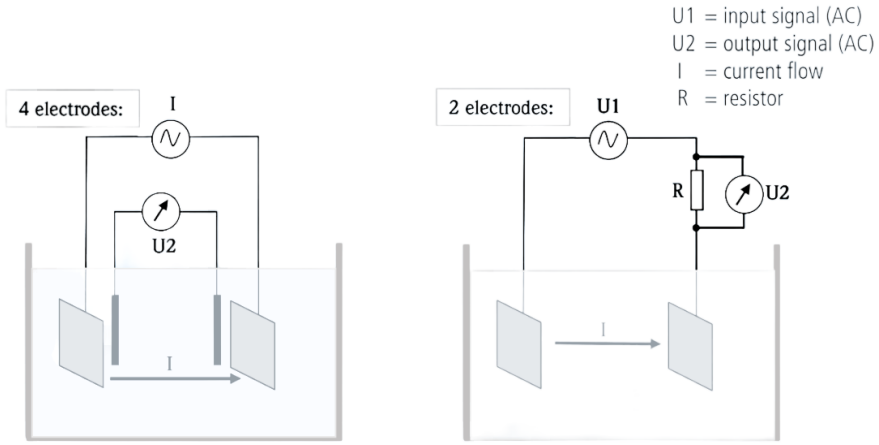

Figure 20. Four electrodes used to measure the conductance, two current electrodes and two measuring electrodes [24]

$$R = \frac{V}{I} \tag{4}$$

Among the various materials utilized for electrode construction, platinum stands out as one of the most widely used due to its excellent conductive properties, biocompatiblity and resistance to corrosion [27]. Their non corrosive nature ensures long-term stability and precision, preventing degradation or oxidation that interfere with accurate conductance measurements. This consistent surface integrity means they provide consistent readings, minimizing variations that arise from electrode surface changes.

3 Chamber

The study and quantification of reactive species in solutions requires a chamber specifically designed to ensure a controlled and optimal environment. Thanks to its carefully considered design and manufacturing, the chamber facilitates seamless integration with the conductivity sensor, enabling accurate and consistent real-time evaluations of reactive species.

3.1 Design

The chamber is designed in Autodesk Fusion 360, allowing a precise and customized approach to its structure. *Figure 21* shows the specific dimensions, ensuring that the volume and flow dynamics of the solution are optimal for measurements. While a large volume is not imperative, it's essential to maintain a consistent volume over an extended period. This consistent volume ensures the stability of readings, allowing for prolonged monitoring without the need to frequently replenish the solution.

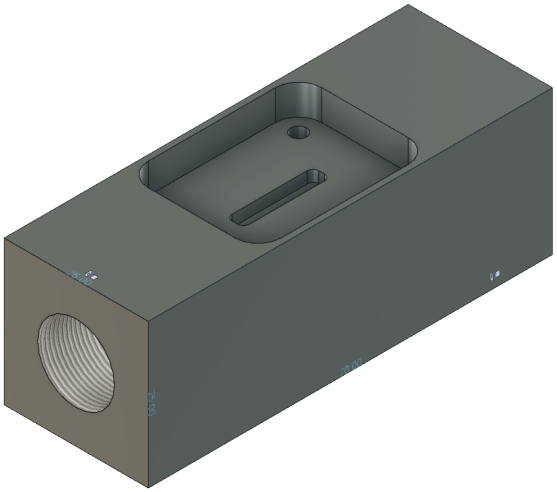

Figure 21. 70.00 mm x 25.00 mm x 25.00 mm rectangular chamber dimensions

Building on this design principle, the chamber's inlet and outlet are meticulously crafted to promote laminar flow, shown in *Figure 22*, reducing turbulence and further enhancing the chamber environment's stability.

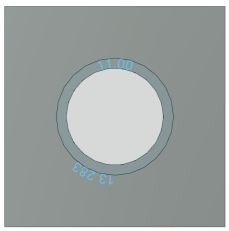

Figure 22. Internal perforation of 11.00 mm through which the PAW will circulate and external perforation of 13.283 mm through which the connector will be threaded

Additionally, the chamber incorporates a large opening for the conductivity sensor's insertion[1]. This opening not only prevents potential leaks but also ensures the sensor's optimal immersion depth, a critical factor for accurate conductivity measurements. Furthermore, the chamber has been designed with strategically placed perforations to facilitate the secure attachment of a cover, adding an additional layer of versatility and adaptability to the overall design. Observe the top and bottom view of the chamber in *Figure 23*.

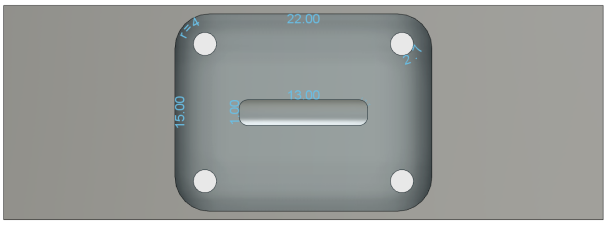

(a) Top of the chamber

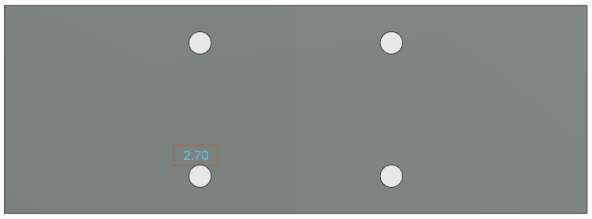

(b) Bottom of the chamber

Figure 23. 13.00 mm x 1.00 mm sensor opening, 2.7 mm diameter perforations for the screws and 22.00 mm x 15.00 mm cover attachment

The cover, shown in *Figure 24* is meticulously designed to be seamlessly integrated into the camera's primary structure, allowing for quick and efficient replacement. The reason for a removable cover is to allow for possible future sensor replacements or upgrades. By ensuring that the cover can be easily replaced, the need for extreme modifications to the camera when changing the sensor is avoided.

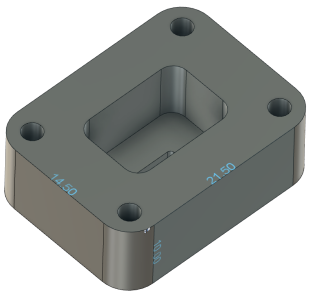

Figure 24. 21.50 mm x 14.50 mm x 10.00 mm cover dimensions

[1]The aperture is deliberately large to allow the use of any other sensor in the future

The design of the cover is slightly smaller than the opening in the chamber. The dimensions observed in *Figure 25* facilitate its easy insertion and removal as needed, providing flexibility in handling and potential replacements or adjustments.

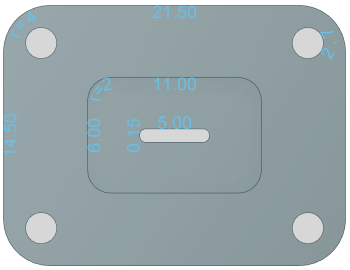

(a) Top of the cover

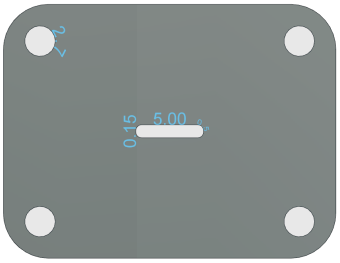

(b) Bottom of the cover

Figure 25. 5.00 mm x 0.15 mm conductivity sensor opening, 11.00 mm x 6.00 mm inner opening, 21.50 mm x 14.50 mm cover edge and 2.7 mm diameter perforations for the screws

In *Figure 26*, all the components of the design are presented, including the chamber, the cover, and the specifically selected connectors and screws. This integrated visualization offers a comprehensive perspective of the entire assembly, illustrating how each part integrates with the others, ensuring a cohesive and functional unit.

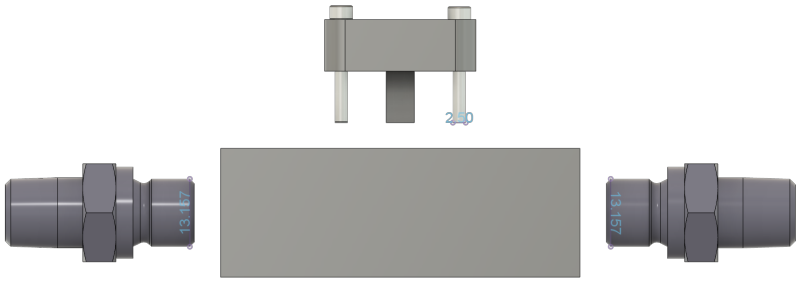

Figure 26. Components of the chamber

As can be observed in *Figure 27*, the height of the cover is intentionally designed to be slightly higher than the hole it covers on the camera. This design decision ensures that when the screws are tightened with considerable force to secure the cover to the camera, the cover will not deform. Maintaining the integrity of the cover is crucial to ensure its long-term

functionality and to avoid any potential damage to the sensor inside. Furthermore, the opening for the conductivity sensor is designed with precision to ensure a perfect fit, allowing the possibility of firmly adhering it in place. The surrounding region of this opening is recessed to a lower profile. This design feature facilitates access and handling of the connections required for the sensor, ensuring its operation and maintenance

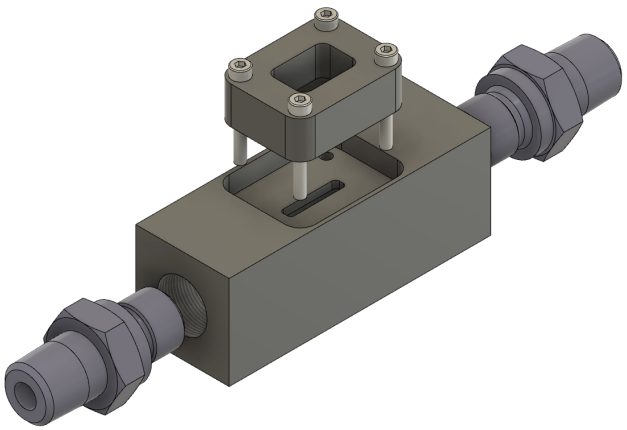

(a) Separate parts of the chamber

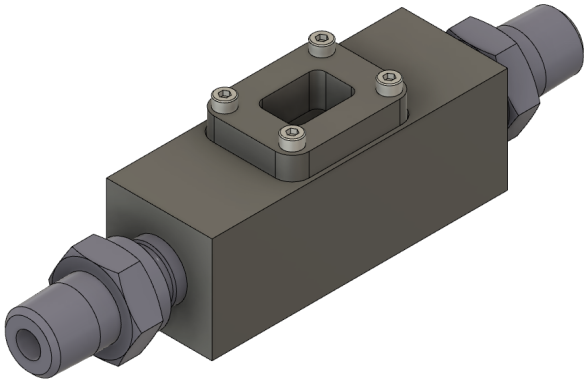

(b) Every part fit together

Figure 27. The principal measurement system and its cover with the screws and two connectors to fit the tube

3.2 Manufacture

The chamber is constructed from PTFE, commonly known as Teflon (as can be observed in *Figure 28*) for its exceptional chemical inertness. This process ensures strict adherence to design specifications while also guaranteeing minimal interference and optimum conditions during measurements.

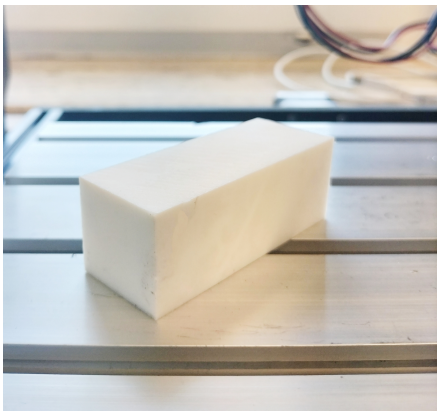

Figure 28. Teflon block

On one hand, in the Teflon block, the inlet and outlet of the measuring system, as shown in *Figure 29*, are made with a bench drill[2]. This method is chosen despite its lack of precision, as the CNC machine lacked drills long enough for this particular operation.

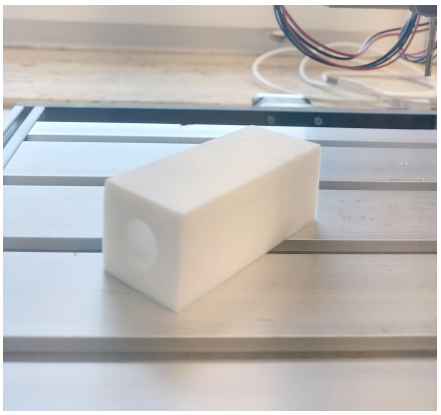

Figure 29. Chamber inlet in Teflon block

On the other hand, the drill holes for the cover attachment and sensor insertion are approached differently. The EAGLE software, shown in *Figure 30*, produces a custom design to guide the CNC machine, ensuring accuracy and precise alignment of these openings in *Figure 31*.

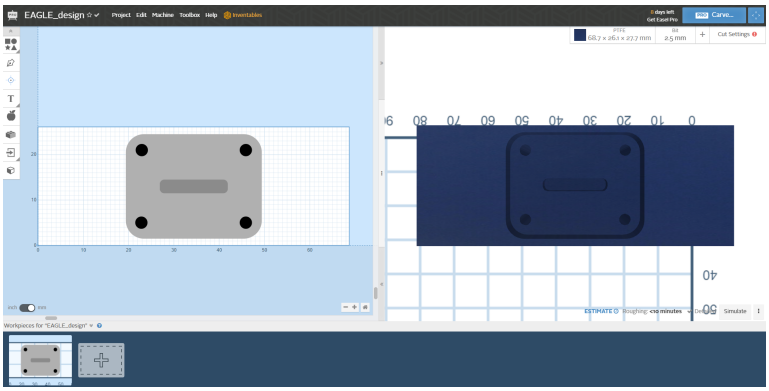

Figure 30. From left to right, the top view of the 2D and 3D design, respectively

[2]See the one used in *Figure 58*, Appendix 1

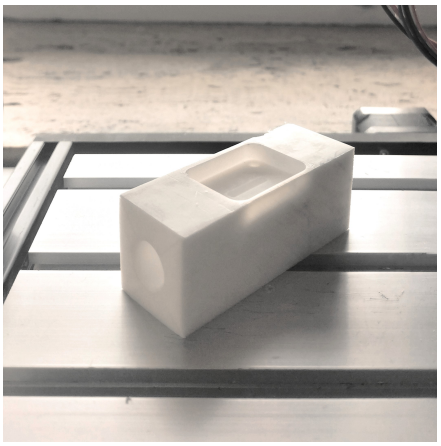

Figure 31. Chamber inlet and cover opening in Teflon block

Meanwhile, the cover, as illustrated in *Figure 32*, is not constructed from the same material as the chamber. Instead, it is manufactured using a 3D printer, employing PLA as the chosen material. PLA is a thermostatic polymer, known for its malleability and ease of fabrication. This choice of material offers versatility, ensuring that if there are future adjustments or replacements of sensors, the cover can be conveniently redesigned and printed without significant challenges.

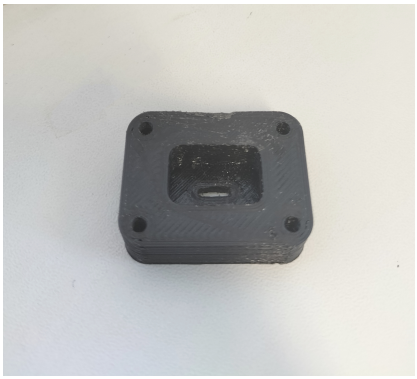

Figure 32. Cover manufactured with a 3D printer

The chosen insulating material to separate the PAW from the rest of the electronic, positioned between the chamber and the cover, as can be observed in *Figure 33*, is Viton.

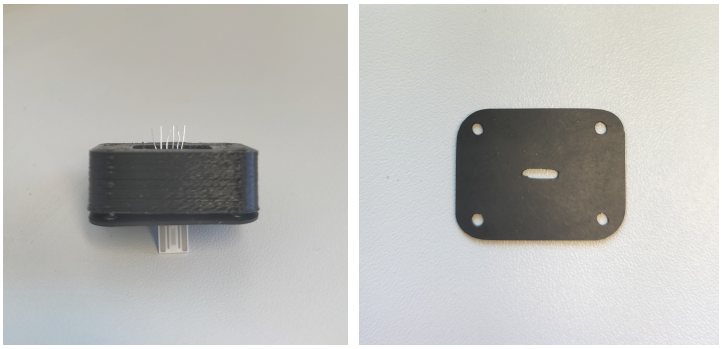

(a) Conductivity sensor glued in the cover

(b) Viton material

Figure 33. PAW isolation from the rest of the electronic

The Viton material, tailored to the exact dimensions of the assembly, is precisely cut using a cutting plotter[3]. Observe in *Figure 34* the Silhouette Cameo 4 software.

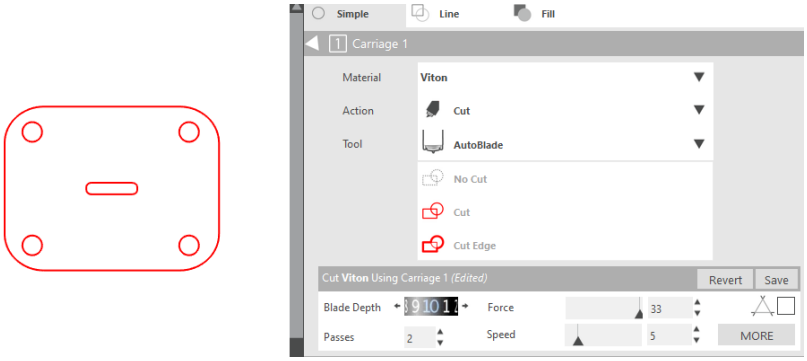

Figure 34. From left to right, design and cutting settings in Silhouette Cameo 4 software, respectively

Finally, the chamber with all components incorporated looks as in the *Figure 35*.

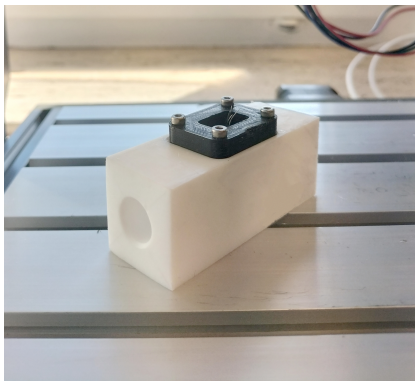

Figure 35. Chamber with all components incorporated

3.3 Sensor installation

Before gluing the sensor to the housing, the legs have to be soldered to a plate, as shown in *Figure 36*, through which the PCB is connected to collect the measurements.

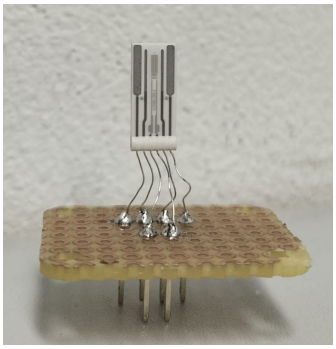

(a) Conductivity sensor soldered to the board

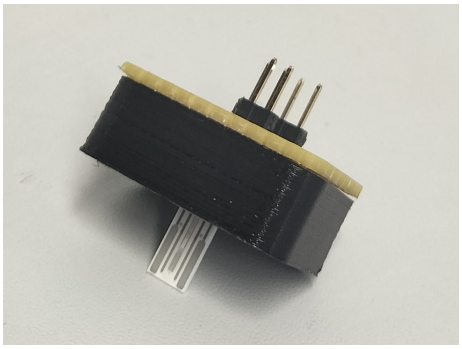

(b) Conductivity sensor glue in the cover

Figure 36. The two front legs are connected to the Pt1000 temperature sensor, while on the four back legs, the end ones correspond to the current electrodes and the other two to the measuring electrodes

[3]Observe the one used in *Figure 59*, Appendix 1

The conductivity sensor is installated in the middle of the path way to effectively measure the PAW as it passes through the measurement system. In *Figure 37*, the sensor is secured and sealed well to prevent leaks.

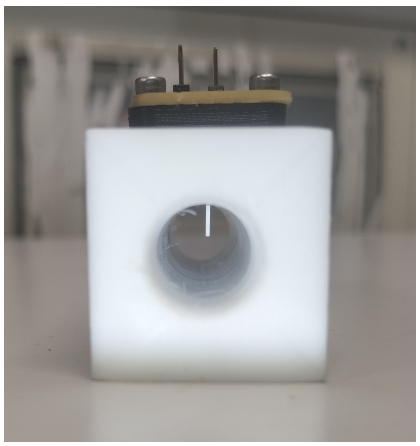

Figure 37. Conductivity sensor installated in the middle of the path way

4 Measurements collection

Ingenious measures are taken to ensure a level of accuracy and reliability suitable for generating and measuring PAW, despite the laboratory environment not being equipped with state-of-the-art instrumentation.

4.1 Measurement System

A paramount component of the measurement system is the plasma gas generator, observe in *Figure 38*, which is responsible for producing the plasma gas that is subsequently introduced into the water sample. When water undergoes plasma treatment, RONS dissolve into it. These species then react with each other and with the water, leading to the emergence of compounds such as H2O2 and OH radicals. The presence and concentration of these reactive species depend on the intensity of the plasma source and the treatment time, resulting in the PAW acquiring an acidic pH [6].

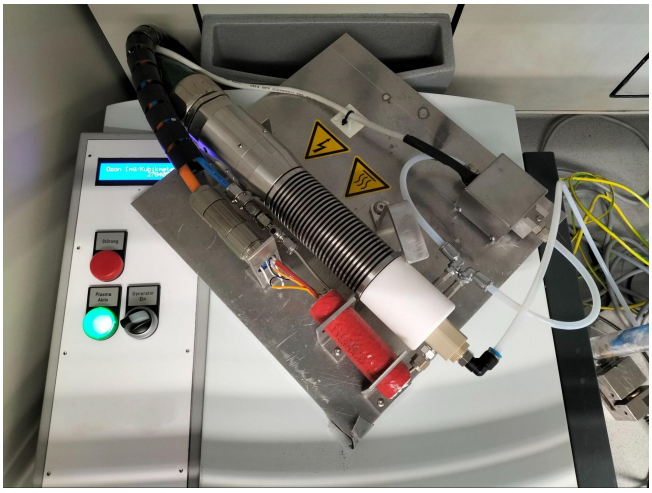

Figure 38. Plasma gas generator

The reactive gas is generated by a plasma system integrated into the stainless steel housing, which, among other things, is composed of an Openair-Plasma nozzle, generator and transformer. After being generated, as can be observed in the scheme in *Figure 39*, the plasma gas is injected into a glass container filled with water [6].

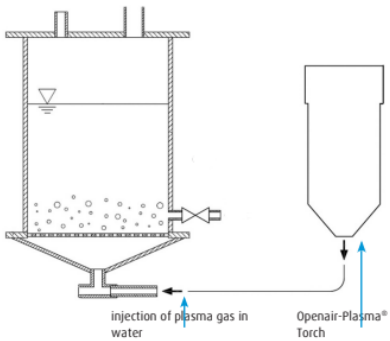

Figure 39. Plasma gas output and injection in a water glass container

In addition to the reactive plasma generator, the measurement system shown in *Figure 40* consists of an air compressor that injects compressed air[1], at pressure of three bar, into a filter responsible for filtering out unwanted components such as oil particles. Next, a flow of thirty liters per minute of compressed air passes through a plasma generator, where a flow of six liters per minute of gas charged with reactive species is produced. Finally, this generated plasma gas passes through a silencer that eliminates some of the unwanted noise[2] before being injected into a two thousand milliliters DI water[3] glass container for the creation of PAW.

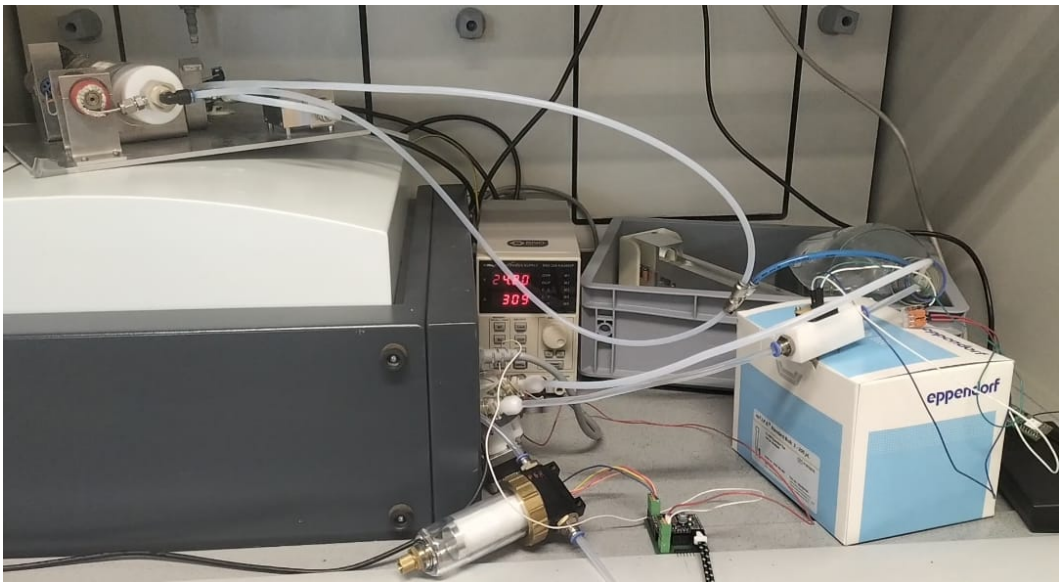

Figure 40. Complete measurement system except the air compressor

The PAW is kept in constant motion through a closed circuit, thus enabling ongoing control of the species generated in the DI water over time. The water's motion is due to the motor integrated into a pump, which is powered by a twenty-four Volts supply and is programmed at a frequency of twenty thousand pulses per second[4], the current speed of the motor. Next, the circulating PAW passes through the chamber, previously designed and manufactured, with the integrated conductivity sensor. The sensor measurements then are collected in the database over time, thanks to the sensor connections established with the PCB.

All components of the measurement system can be seen in *Figure 41*.

[1]For it to work properly, the air conditioner is turned on

[2]Related to the plasma generation process and the interaction between the reactive gas and DI water

[3]This quantity is very important for the amount of reactive species that are generated in the DI water

[4]The exact frequency so that the liquid circulates and no air is produced to introduce noise into the measurements

(a) Air compressor

(b) Inside pressure ≈ 3 Bar

(c) Outlet pressure ≈ 3 Bar

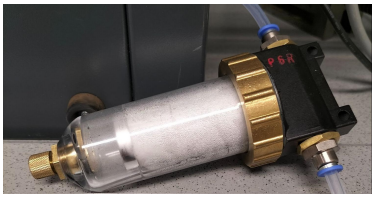

(d) Filter

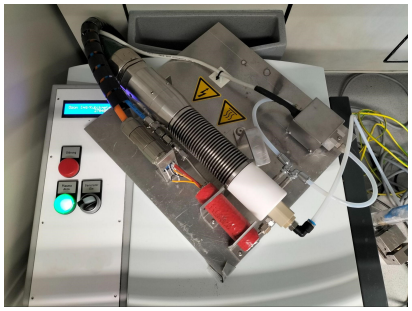

(e) Plasma generator

(f) Silencer

(g) DI water glass container

(h) Power supply

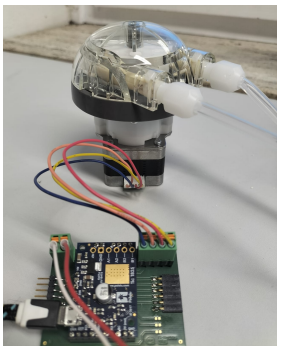

(i) Pump

(j) Chamber

Figure 41. Components of the measurement system

4.2 Data collection

Before starting data collection with the conductivity sensor, it is necessary to test it and calibrate it. For this purpose, the pump motor is switched on so that DI water starts to circulate through the measuring system without the injection of plasma gas. For ten minutes, the sensor is collecting measurements, where the average resistance is 259883 Ohms, resulting in zero conductance, as can be seen in *Figure 42*.

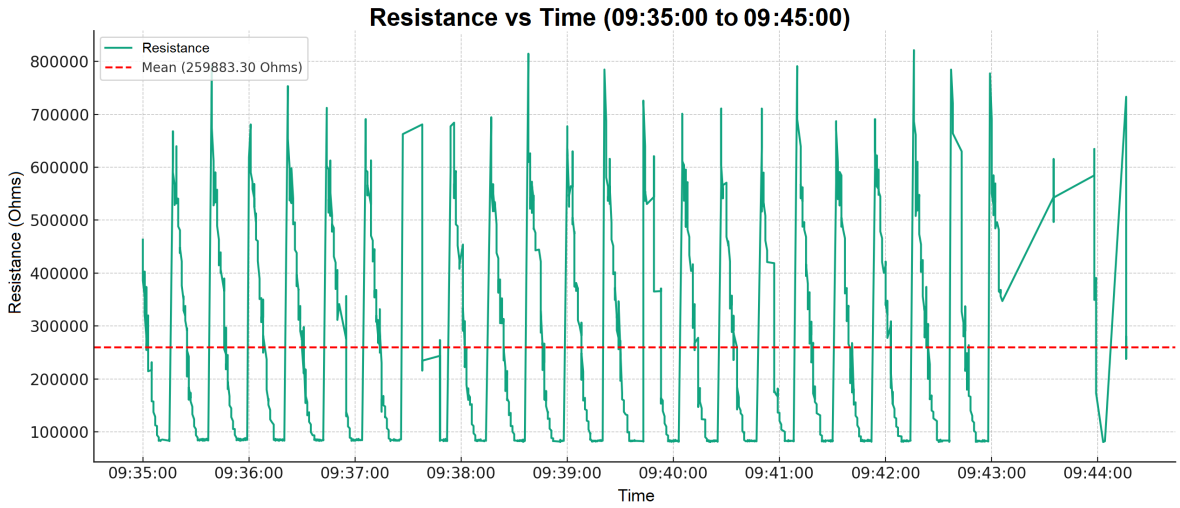

(a) Resistance readings

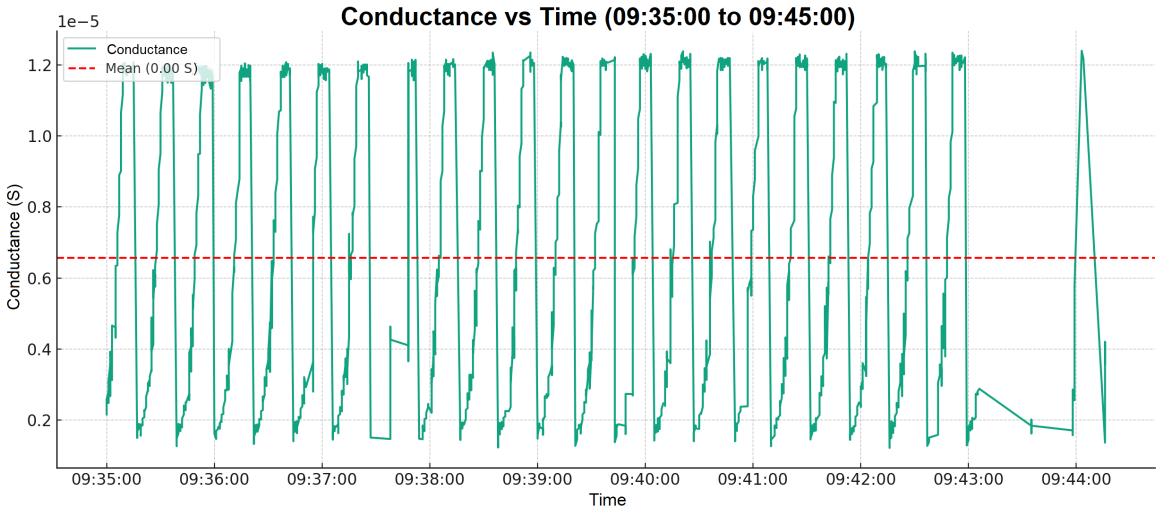

(b) Conductance readings

Figure 42. Calibration of the conductivity sensor for ten minutes

The sensor is working correctly, the mean conductance value is zero because the DI water is not able to conduct electric current, as there are no dissolved reactive species yet. This is also verified with the reference sensors, the multi-parameter tester and the TDS sensor, in Chapter 2. Sensors. In addition, it is checked that there are no leaks in the measurement system and that no additional adjustments are needed.

Once the measurement system is configured and calibrated, the plasma generator is turned on to start injecting gaseous plasma into the glass container with water. As can be seen in *Figure 43*, the conductivity sensor is reading values for one hour.

The conductance of the solution increases progressively with exposure to the reactive gas, although there are inconsistencies due to sampling every ten minutes for measurement with the reference sensors. To show the general direction in which the conductance values change as time passes, a regression line is plotted. While the positive slope indicates the rate at which the conductance increases, the ordinate at the origin indicates practically zero conductance when the experiment is not started, i.e. when the amount of added reactive gas is zero.

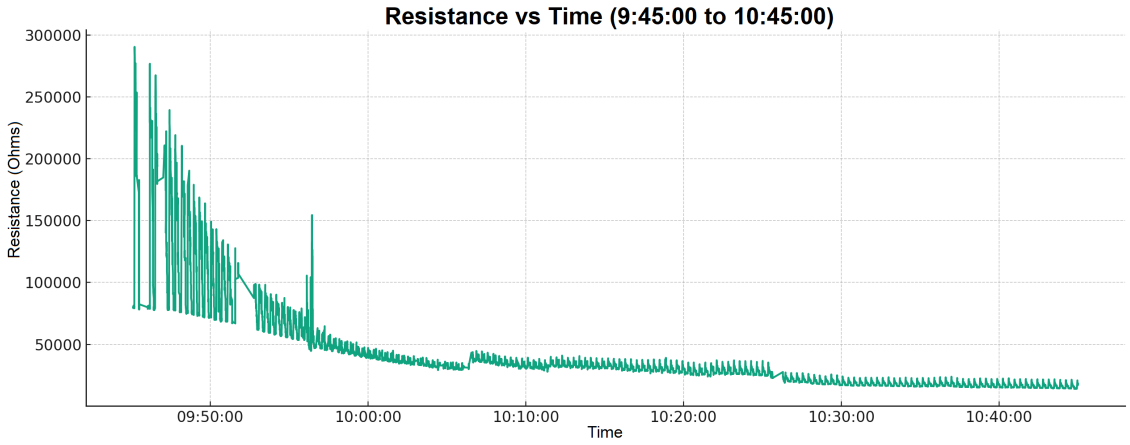

(a) Resistance readings

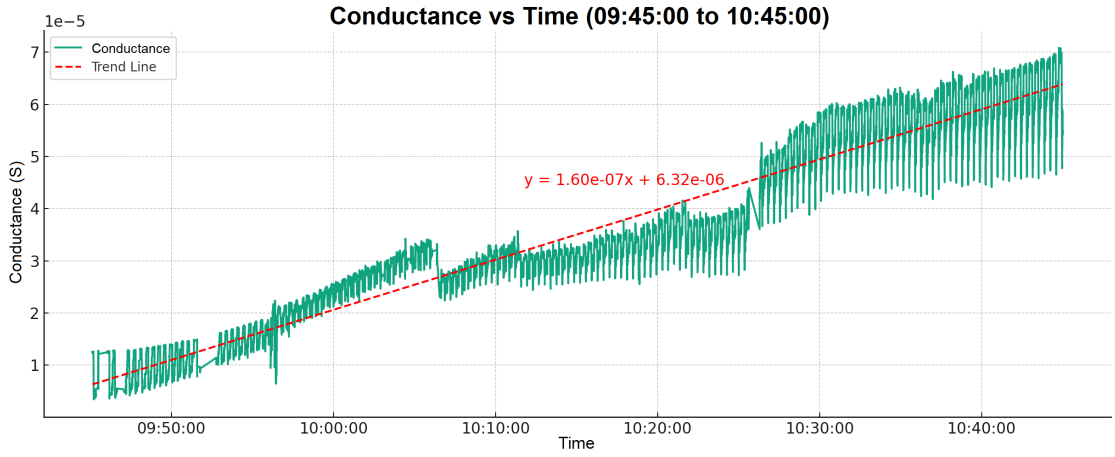

(b) Conductance readings

Figure 43. Conductivity sensor readings for an hour

If the same measurements are plotted with respect to the gas added at a rate of six liters per minute, as can be seen in *Figure 44*, a total of approximately three hundred sixty liters of added reactive gas is generated during the experiment.

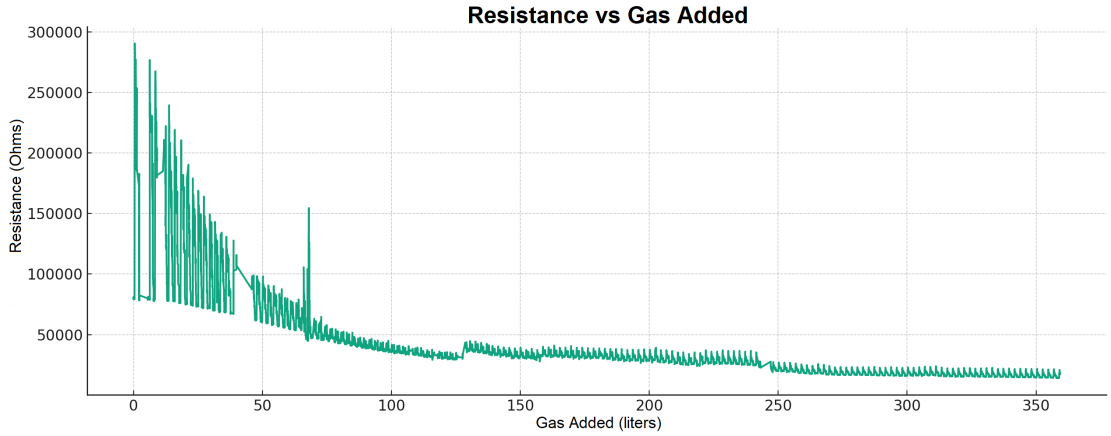

(a) Resistance readings

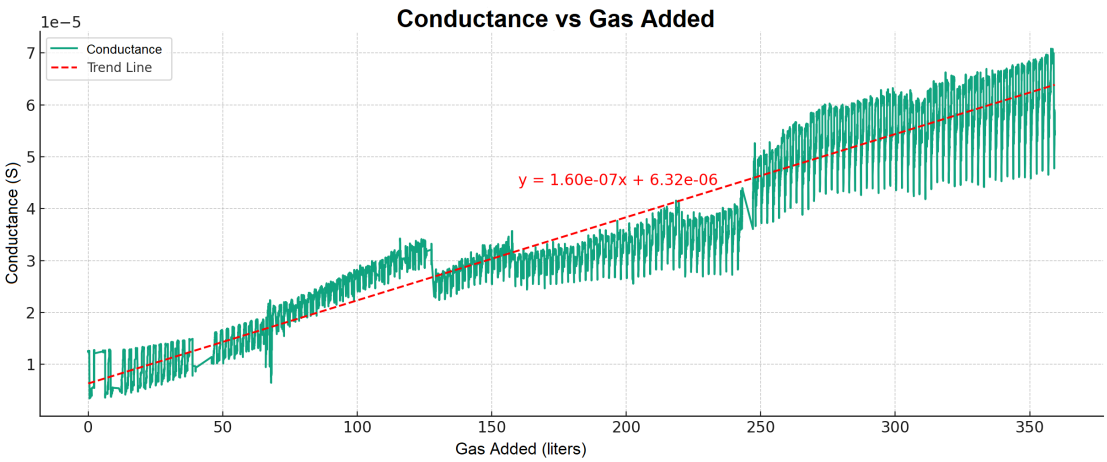

(b) Conductance readings

Figure 44. Conductivity sensor readings when six liters of reactive gas is added per minute

4.3 Data validation

The readings obtained with the conductivity sensor cannot be analyzed yet, because they are not reliable. Therefore, these data must be validated with the reliable standard sensors seen in Chapter 2. Then, a sample of the solution is taken every ten minutes during the experiment, a total of 7 samples. The conductivity sensor readings are sampled in *Figure 45*.

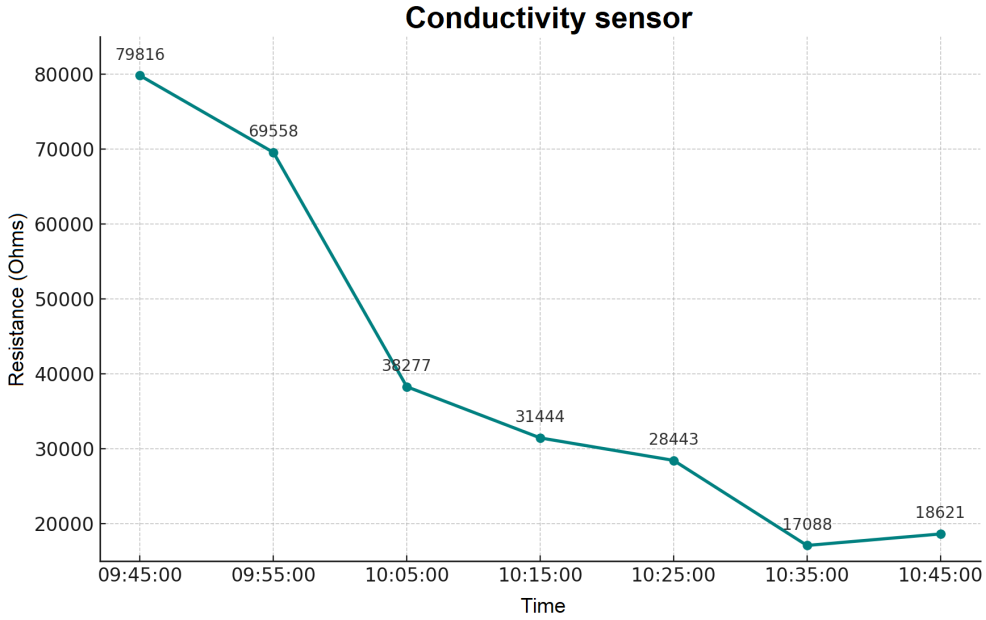

(a) Resistance samples

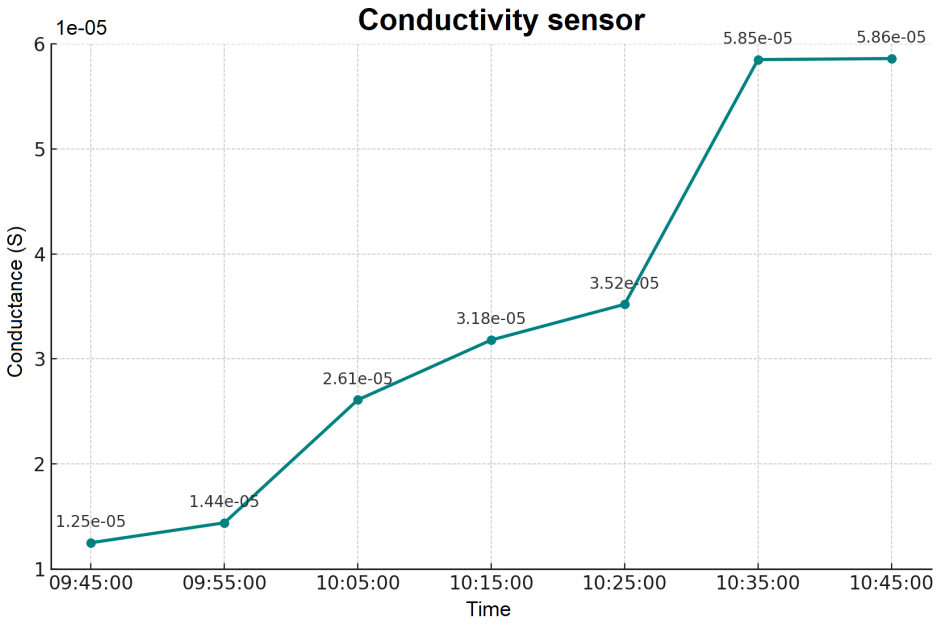

(b) Conductance samples

Figure 45. A sample of conductivity sensor readings every ten minutes

In turn, the readings obtained by the reference sensors at the same time are as shown in *Figure 46* and *Figure 47*. With the TDS sensor, from the TDS values read, the conductivity is calculated with *Equation 1* and factor *k* equal to 0.47, as seen in Chapter 2. Sensors.

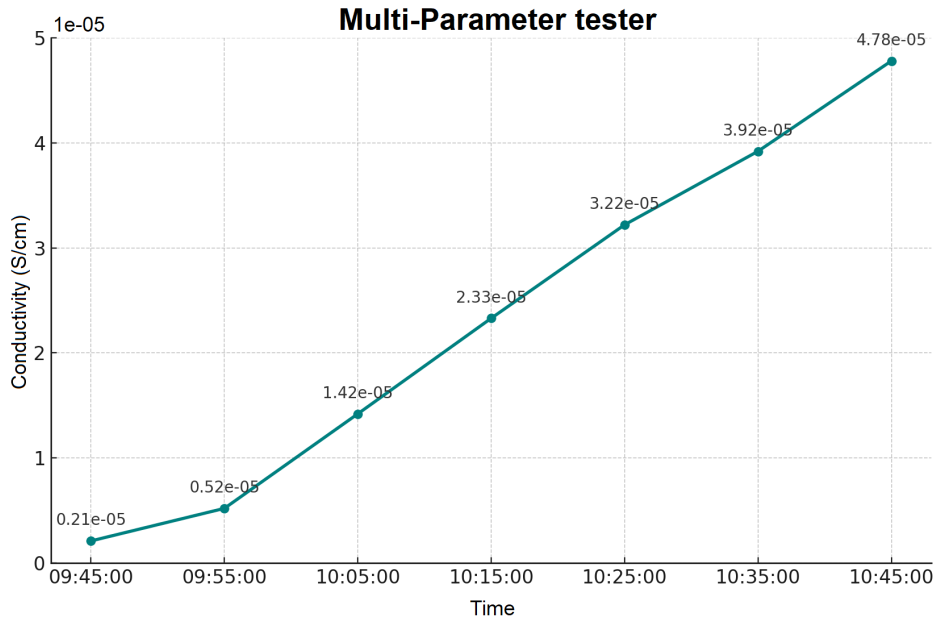

(a) Conductivity samples

Figure 46. A sample of multi-parameter tester readings every 10 minutes

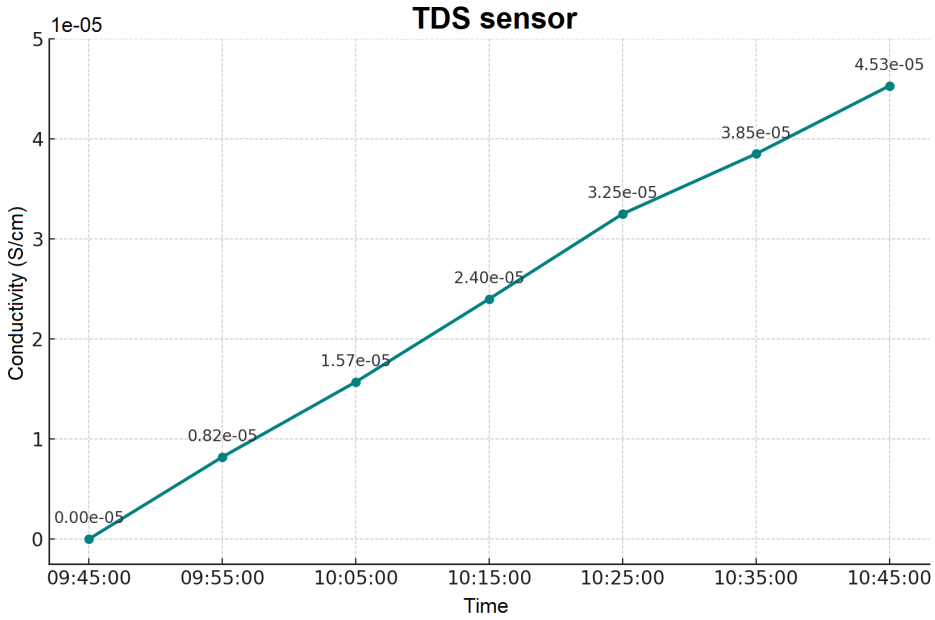

(a) Conductivity samples

Figure 47. A sample of TDS sensor readings every ten minutes

It can be observed that the values are not comparable, but they follow the same trend, as time goes by both conductance and conductivity increase with similar values. However, these values never coincide because in the case of the conductivity sensor, the surface on which the measurements are being taken is not being taken into account. Whereas with the reference sensors, the surface on which the measurements are being taken is taken into account.

4.4 Data discussion

At the same time the samples are being measured with the reference sensors, a semi-quantitative test strip for peroxide 25 is being used[5], like the strip sensitivity, to measure the approximate concentration of hydrogen peroxide. When the test strip is introduced inside the PAW, the substance test strip reacts with the peroxide producing a color change. The intensity of the color change is proportional to the concentration of peroxide in the solution. According to the manufacturer, the solution can go from zero point five mg/L to twenty-five mg/L of peroxide 25. As can be seen in the *Figure 48* of the test strips introduced every 10 minutes in the samples, the concentration of peroxide hydrogen is very small.

The small amount of species generated in the process, solution with low electric properties, may be due to the large amount of DI water at the start, there are few dissolved species in a lot of water. As possible solutions, less water is taken or a higher circulation speed of the motor is used, which increases the number of bubbles and in turn the noise of the system. In addition, it is found that the direction of the motor also influenced the generation of bubbles, so that some part of the chamber design allowed air to pass through. Moreover, the previous graphs show that the measurements collected are accompanied by noise that can be caused by a turbulent flow type, either due to edges, sticking to walls, etc. Therefore, if measurements are collected in a measuring system in which a turbulent flow is generated, versus measurement

[5]Observe it in *Figure 60*, Appendix 1

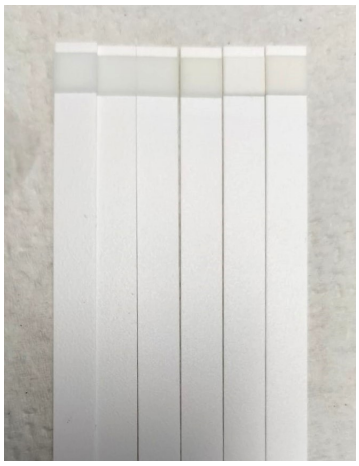

Figure 48. Semi-quantitative test each ten minutes, from right to left

in a specimen in which no flow is generated, a laminar flow, the measured electrical property changes.

It is also observed that as the electric properties increase, temperature tends to decrease. Theoretically, as more reactions occur within a solution, the particles exhibit greater movement, generating heat. However, in the experimental context, it is believed that the influence of the ambient temperature, 22°C, contributes to the PAW generated becoming closer and closer to room temperature, reaching thermal equilibrium.

It would be perfect to have as many reactive species as possible available for prophylaxis in surgery. However, it is not yet known whether this is possible or whether is come a time when no more reactive species are generated and these are insufficient for the application. More research is needed.

5 Conclusions

The main objective of the project is to address the feasibility and functionality of a system for monitoring reactive species in PAW. For this purpose, it is been possible to compare the measured values of the species generated using different detection methods.To achieve this, a series of experimental procedures involving several stages are carried out.

Initially, during the start of the project, an extensive learning phase is carried out to understand two different sensors to collect data in various solutions, their calibration and initial evaluation. These sensors, known for their accuracy and reliability, serve as a reference for comparison with the conductivity sensor. This preliminary work with the sensors serves as the basis for the final reactive species accurate monitoring system. After this initial phase, the design and fabrication of the chamber that integrates the conductivity sensor begins. The chamber is designed with shape and dimensions in mind, for uniform flow distribution and minimum turbulence. However, the lack of precision of the tools used for its manufacture means that the flow is not distributed as originally intended, producing interferences but ensuring that the functionality of the measurement system is met.

Coinciding with the completion of the above tasks, the plasma generation equipment arrives at the company. Taking advantage of the occasion, the equipment is installed and configured together with the rest of the measurement system. Measurements are made with the conductivity sensor, passing the solution with the reactive species through a closed system. The performance of the measurement system is validated, although not entirely accurate, more measurements and research should be done. For instance, incorporating an optical detection system, exemplified by an optical probe functioning as an additional electrode, could yield substantial advantages. The integration of such an optical probe has the potential to exert influence over the generation of reactive species in PAW. By considering the implementation of UV LEDs in conjunction with an optical instrument, it becomes plausible to employ it as a detector for H2O2 species, thereby broadening the capabilities of the measurement system.

References

[1] Francis A. P. Ake Oberg, Tatsuo Togawa. *Sensors in Medicine and Health Care*. Weinheim;Wiley-VCH, 2004.

[2] Universidad de Tarapacá. *Sensores y transductores*. Universidad de Tarapacá, 2023.

[3] Antonio Del Brío García. *Tecnología electrónica en ingeniería biomédica: sensores*. Universidad de Valladolid, 2020.

[4] Hao Wan. *Biomedical sensors*. ScienceDirect, 2020.

[5] Juan Mulundi. *The Introduction to Biomedical Instrumentation*. Biomedical Instrumentation Systems, 2020.

[6] Mitrovics Jan Wallner Michael, Schmitt-John Thomas. *Project description for the implementation of a project within the framework of VWW Invest BW - Innovation II*. Invest BW, 2022.

[7] Milosavljevic C Pejovic M, Markovic V. Separation of ionic and metastable contributions to breakdown initiation in nitrogen. *Journal of Physics D: Applied Physics*, Volume 24(5):677–680, 1991.

[8] Michael Keidar Dayun Yan1, Jonathan H. Sherman2. *Cold atmospheric plasma, a novel promising anti-cancer treatment modality*. Oncotarget, 2017.

[9] Kim Chul-Ho Kim Sungyeol. Applications of plasma-activated liquid in the medical field. *National Library of Medicine*, Volume 9(11), 2021.

[10] E Wagenaars. *Plasma breakdown of low-pressure gas discharges*. Technische Universiteit Eindhoven, 2006.

[11] A.Hecimovic J.T.Gudmundsson1. *Foundations of dc plasma sources*. Iceland, Sweden and Germany Universities, 2017.

[12] Boehm Daniela Tsoukou Evanthia, Bourke Paula. Temperature stability and effectiveness of plasma-activated liquids over an 18 months period. *International Journal of Molecular Sciences*, Volume 12(11), 2020.

[13] Moreira Milhan Noala Vicensoto da Graça Sampaio Aline, Chiappim William et al. Effect of the ph on the antibacterial potential and cytotoxicity of different plasma-activated liquids. *International Journal of Molecular Sciences*, Volume 23(22), 2022.

[14] Wang Peiyu Zhou Renwu, Zhou Rusen and Xian Y. Plasma activated water (paw): generation, origin of reactive species and biological applications. *Journal of Physics D Applied Physics*, Volume 53(30), 2020.

[15] Prasad Karthika Zhou Renwu, Zhou Rusen et al. Cold atmospheric plasma activated water as a prospective disinfectant: the crucial role of peroxynitrite. *Green Chemistry*, 2018.

[16] Patange Apurva Zhao Yunlu, Lokesh Bhavya Mysore et al. Plasma-activated liquids for mitigating biofilms on food and food contact surfaces. *Journal of Food Science*, 2023.

[17] Annapure Uday Thirumdas Rohit, Kothakota Anjinelyulu et al. Plasma activated water (paw): Chemistry, physico-chemical properties, applications in food and agriculture. *Science Direct*, Volume 77:pages 21–31, 2018.

[18] Woedtke Thomas von Jablonowski Helena. Plasma-liquid interaction research relevant to plasma medicine: what happened in the last five years? *Clinical Plasma Medicine*, 2015.

[19] Isahit blog. What is sensor calibration and why is it important? https://www.isahit.com/blog/what-is-sensor-calibration-and-why-is-it-important.

[20] Apera Instruments. Pc60 premium 5-in-1 multi-parameter pocket meter. https://aperainst.de/produkt/pc60-premium-5-in-1-multi-parameter-measuring-device-ph-value-conductivity-tds-salt-content-temperature/?lang=en.

[21] LLC APERA INSTRUMENTS. *PC60 Premium Multi-Parameter Tester (pH/EC/TDS/Salinity/Temp.). Instruction Manual*. Apera Instruments.

[22] Apera Instruments Official Channel. *How to calibrate Apera Instruments 60 Series Premium pH Testers (1-3 points calibration)*. Apera Instruments Official Channel, 2016.

[23] CQRobot-Wiki. Tds (total dissolved solids) meter sensor sku: Cqrsentds01. http://www.cqrobot.wiki/index.php/TDS_(Total_Dissolved_Solids)_Meter_Sensor_SKU:_CQRSENTDS01.

[24] Dr. Florian Krogmann. *Conductivity Sensors*. Innovative Sensor Technology.

[25] Springer Nature. Plasma chemistry and plasma processing. https://www.researchgate.net/figure/Concentration-of-nitrite-nitrate-and-hydrogen-peroxide-in-water-as-function-of-plasma_fig4_355173312.

[26] Martinsen G Grimnes S. *Electrodes*. Bioimpedance and Bioelectricity Basics, 2015.

[27] Szmigiel D Grabiec P, Domanski K and Hodgins D. *Electrode array design and fabrication for implantable systems*. Implantable Sensor Systems for Medical Applications, 2013.

A Appendix 1. Additional figures

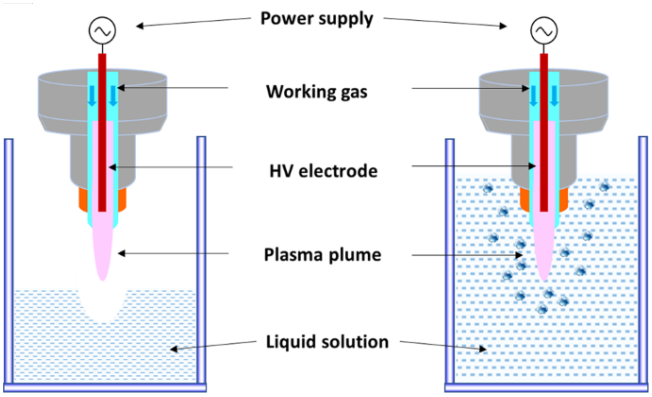

Figure 49. On the left, under the non-touch conditions, RONS are initially generated in the gaseous plasma and only long-lived RONS can subsequently dissolve and enter the solution. On the right, in the direct contact mode, apart from the accumulation of the reactive species from the gas-phase plasma, numerous additional reactive species are generated through plasma-liquid interactions in the solution

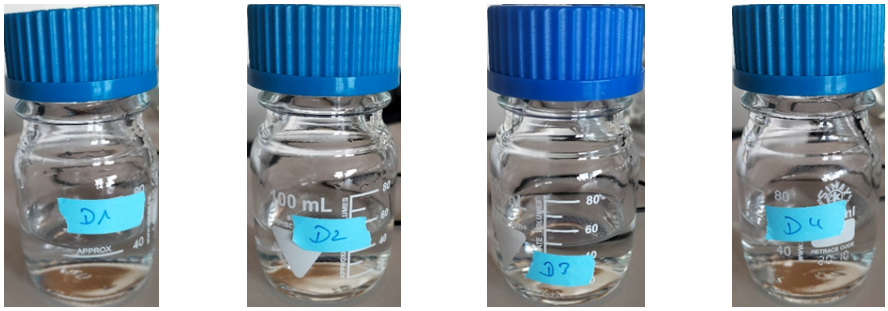

(a) Dilution 1 (b) Dilution 2 (c) Dilution 3 (d) Dilution 4

Figure 50. Fifty milliliters PAW dilutions

Conductivity	Range	0 to 200.0 uS, to 2000 uS, 0 to 20.00 mS/cm
	Resolution	0.1/1 uS, 0.01 mS/cm
	Accuracy	±1% F.S
	Calibration Points	1 to 3 points
pH	Range	-2.00 to 16.00 pH
	Resolution	0.01 pH
	Accuracy	±0.01 pH ± 1 digit
	Calibration Points	1 to 3 points
	Automatic Temperature Compensation	0 – 50 °C (32 –122°F)
TDS	Range	0.1 ppm to 10.00 ppt
	TDS Factor	0.40 to 1.00
Salinity	Range	0 to 10.00 ppt
Temperature	Range	0 to 50°C (32 –122°F)
	Resolution	0.1°C
	Accuracy	±0.5°C

Figure 51. Parameters technical specifications [21]

Figure 52. Default TDS factor in the multi-parameter tester

Figure 53. Conductivity and pH calibration buffer solutions

Input voltage	3.3 V to 5.5 V
Output voltage	0 V to 2.3 V, compatible with 5V or 3.3V controller
Working current	3 mA to 6 mA
TDS range	0 ppm to 1000 ppm
TDS accuracy	±10% F.S. (25°C)
Usage	Arduino compatible
Compatibility	ADS1115 16-bit ADC, Raspberry Pi

Figure 54. Technical specifications TDS meter sensor [23]

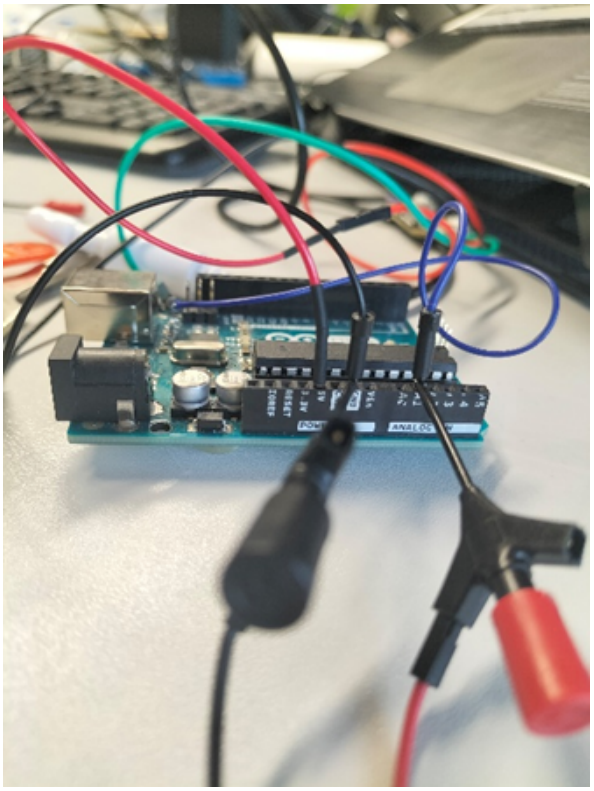

Figure 55. Set up to measure the voltage, with the multimeter, in the microcontroller microchip that is integrated in the Arduino UNO board

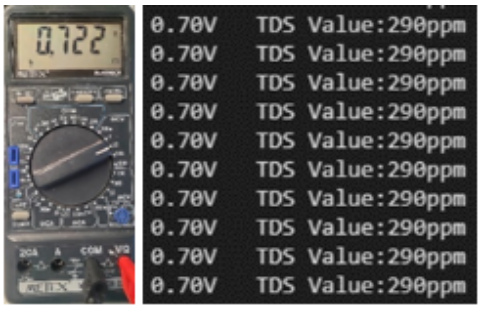

(a) Dilution 1

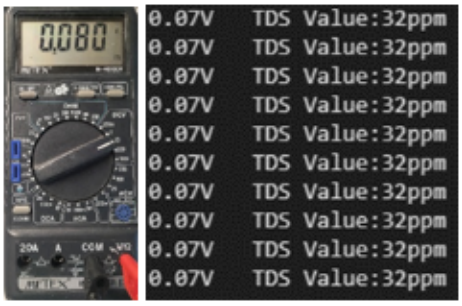

(b) Dilution 2

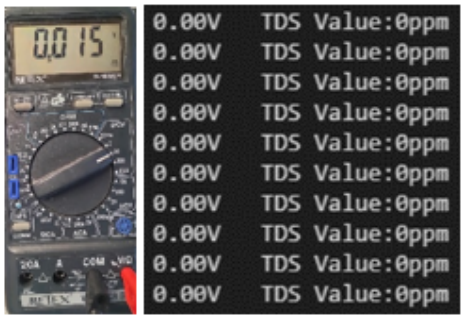

(c) Dilution 3

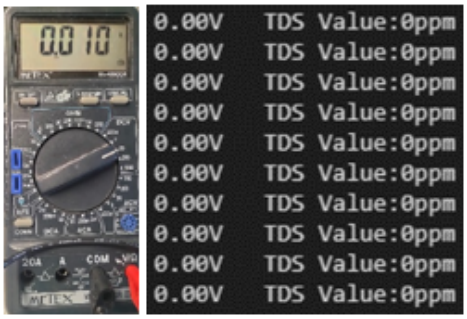

(d) Dilution 4

Figure 56. Voltage and TDS measurements

Dimensions	7 mm x 10 mm x 0.65 mm
Substrate	AI2O3
Working temperature	0 °C … +90 °C
Storage temperature	-20°C … +80 °C
Measuring range of temperature	µS/cm to ~20 mS/cm
Cell constante	typ. 0.41 cm-1 0.2 cm-1 to 0.7 cm-1
Electrodes	Pt100 or Pt1000, DIN EN 60751, Class F 0.3 and Class F 0.15 possible
Connection	Platinum electrodes 6x Ni/Pt wires 0.2 mm, AWG 30, insulated
Measuring frequency	300 to 3000 Hz
Max. voltage load of the current electrodes	1.6 Vpp*

*Without DC component

Figure 57. Conductivity sensor technical specifications [24]

Figure 58. Bench drill

Figure 59. Cutting plotter

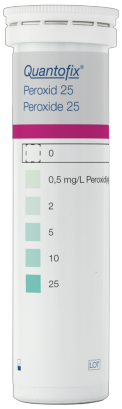

Figure 60. Semi-quantitative test strips for peroxide 25